



Published in final edited form as:

Exp Neurol. 2015 September ; 271: 479–492. doi:10.1016/j.expneurol.2015.07.020.

Human iPS cell-derived astrocyte transplants preserve respiratory function after spinal cord injury

Ke Li^a, Elham Javed^a, Daniel Scura^a, Tamara J. Hala^a, Suneil Seetharam^a, Aditi Falnikar^a, Jean-Philippe Richard^b, Ashley Chorath^a, Nicholas J. Maragakis^b, Megan C. Wright^c, and Angelo C. Lepore^{a,d}

Ke Li: ke.li@jefferson.edu; Elham Javed: elham.javed@jefferson.edu; Daniel Scura: Daniel.scura@jefferson.edu; Tamara J. Hala: tamara.hala@jefferson.edu; Suneil Seetharam: suneil.seetharam@jefferson.edu; Aditi Falnikar: aditi.falnikar@jefferson.edu; Jean-Philippe Richard: jricha68@jhmi.edu; Ashley Chorath: Ashley.chorath@jefferson.edu; Nicholas J. Maragakis: nmaragak@jhmi.edu; Megan C. Wright: wright@arcadia.edu

^aDepartment of Neuroscience, Farber Institute for Neurosciences, Sidney Kimmel Medical College at Thomas Jefferson University, 900 Walnut Street, JHN 469, Philadelphia, PA, 19107, United States

^bDepartment of Neurology, Johns Hopkins University School of Medicine, 855 N. Wolfe St., Rangos 250, Baltimore, MD, 21205, United States

^cDepartment of Biology, Arcadia University, 450 S. Easton Rd., 220 Boyer Hall, Glenside, PA, 19038, United States

Abstract

Transplantation-based replacement of lost and/or dysfunctional astrocytes is a promising therapy for spinal cord injury (SCI) that has not been extensively explored, despite the integral roles played by astrocytes in the central nervous system (CNS). Induced pluripotent stem (iPS) cells are a clinically-relevant source of pluripotent cells that both avoid ethical issues of embryonic stem cells and allow for homogeneous derivation of mature cell types in large quantities, potentially in an autologous fashion. Despite their promise, the iPS cell field is in its infancy with respect to evaluating *in vivo* graft integration and therapeutic efficacy in SCI models. Astrocytes express the major glutamate transporter, GLT1, which is responsible for the vast majority of glutamate uptake in spinal cord. Following SCI, compromised GLT1 expression/function can increase susceptibility to excitotoxicity. We therefore evaluated intraspinal transplantation of human iPS cell-derived astrocytes (hIPSA) following cervical contusion SCI as a novel strategy for reconstituting GLT1 expression and for protecting diaphragmatic respiratory neural circuitry. Transplant-derived cells showed robust long-term survival post-injection and efficiently differentiated into astrocytes in

^d**Corresponding author:** Angelo C. Lepore, Ph.D., Department of Neuroscience; Farber Institute for Neurosciences, Sidney Kimmel Medical College at Thomas Jefferson University, 900 Walnut Street, JHN 469, Philadelphia, PA 19107, Phone: 215-503-5864; Fax: 215-955-4949, angelo.lepore@jefferson.edu.

Publisher's Disclaimer: This is a PDF file of an unedited manuscript that has been accepted for publication. As a service to our customers we are providing this early version of the manuscript. The manuscript will undergo copyediting, typesetting, and review of the resulting proof before it is published in its final citable form. Please note that during the production process errors may be discovered which could affect the content, and all legal disclaimers that apply to the journal pertain.

Contributions

KL: Conception and design, collection and assembly of data, data analysis and interpretation, manuscript writing. EJ, TJH, SS, MCW: Collection and assembly of data, data analysis and interpretation. JPR, NJM: Provision of study materials. ACL: Conception and design, collection and assembly of data, data analysis and interpretation, manuscript writing, final approval of manuscript.

injured spinal cord of both immunosuppressed mice and rats. However, the majority of transplant-derived astrocytes did not express high levels of GLT1, particularly at early times post-injection. To enhance their ability to modulate extracellular glutamate levels, we engineered hIPSAs with lentivirus to constitutively express GLT1. Overexpression significantly increased GLT1 protein and functional GLT1-mediated glutamate uptake levels in hIPSAs both *in vitro* and *in vivo* post-transplantation. Compared to human fibroblast control and unmodified hIPSA transplantation, GLT1-overexpressing hIPSAs reduced (1) lesion size within the injured cervical spinal cord, (2) morphological denervation by respiratory phrenic motor neurons at the diaphragm neuromuscular junction, and (3) functional diaphragm denervation as measured by recording of spontaneous EMGs and evoked compound muscle action potentials. Our findings demonstrate that hiPSA transplantation is a therapeutically-powerful approach for SCI.

Keywords

induced pluripotent stem cells; cervical spinal cord contusion; astrocyte; glutamate transporter; glial progenitor

Introduction

Transplantation of neural stem cells (NSCs) and neural progenitor cells (NPCs) is a promising therapeutic strategy for both neurodegenerative diseases of the central nervous system (CNS) and traumatic CNS injury, including spinal cord injury (SCI), because of the ability to replace lost and/or dysfunctional nervous system cell types, promote neuroprotection, deliver gene factors of interest and provide other benefits (Gage, 2000).

Initial trauma following SCI results in immediate cell death and axotomy of passing fibers. Contusion- and compression-type injuries, the predominant forms of traumatic SCI observed in the clinical population, are followed by an extended period of secondary cell death and consequent exacerbation of functional deficits (McDonald and Becker, 2003). One of the major causes of secondary degeneration following SCI is excitotoxic cell death due to dysregulation of extracellular glutamate homeostasis (Park et al., 2004; Stys, 2004). Exogenous parenchymal administration of glutamate to uninjured spinal cord results in tissue and function loss similar to SCI (Xu et al., 2005). While large increases in glutamate can occur shortly after SCI, elevation can also persist depending on injury severity (Liu et al., 1991; Panter et al., 1990; Xu et al., 2004). In addition to focal increases, levels can also rise in regions removed from the lesion site, possibly via a spreading mechanism involving activated glia (Hulsebosch, 2008). Early gray matter loss is likely mediated by NMDA receptors, while delayed loss of neurons and oligodendrocytes, as well as axonal and myelin injury, is thought to be predominantly mediated via AMPA over-activation (Stys, 2004). A valuable opportunity therefore exists after SCI for preventing cell injury and functional loss that occur during secondary degeneration. Importantly, secondary degeneration is a relevant therapeutic target given its relatively prolonged time window.

Glutamate is efficiently cleared from the synapse and other sites by transporters located on the plasma membrane (Maragakis and Rothstein, 2004). Astrocytes are supportive glial cells that play a host of crucial roles in CNS function (Pekny and Nilsson, 2005). Astrocytes

express the major CNS glutamate transporter, GLT1, which is responsible for the vast majority of functional glutamate uptake and plays a central role in regulation of extracellular glutamate homeostasis in the spinal cord (Maragakis and Rothstein, 2006). Following SCI, astrocyte loss and/or altered GLT1 expression, function and localization can result in further susceptibility to excitotoxicity. For example, we previously found that in rodent models of unilateral mid-cervical (C4) contusion SCI, numbers of GLT1-expressing astrocytes, total intraspinal GLT1 protein expression and GLT1-mediated functional glutamate uptake in ventral horn are reduced soon after injury and this reduction persists chronically (Li et al., 2014b). Astrocytes have traditionally been viewed in a negative light following CNS trauma because of their association with disease mechanisms such as glial scarring and pro-inflammatory cytokine release. However, their crucial neuroprotective/homeostatic roles, including GLT1-mediated glutamate uptake, have not been extensively targeted in SCI models using approaches such as NSC and NPC transplantation, despite obvious therapeutic implications (Maragakis and Rothstein, 2006).

Transplantation-based targeting of astrocytes provides a number of key benefits. Grafts can be anatomically delivered to precise locations for achieving neuroprotection of specific populations of cells (Lepore et al., 2008b). Alternative strategies such as gene therapy only target one/several specific genes (s), while astrocyte transplantation can participate in the restoration of a host of astrocyte functions. Transplantation also provides for long-term astrocyte integration and therapeutic replacement. For example, the lasting nature of dysregulation of extracellular glutamate homeostasis after SCI (Lepore et al., 2011a; Lepore et al., 2011c) calls for longer-term maintenance of therapeutic effects, both with respect to early cell loss occurring during secondary degeneration and outcomes of SCI associated with more persistent pathophysiology of glutamate signaling such as chronic neuropathic pain (Gwak et al., 2012; Hulsebosch, 2008).

To achieve translation of NSC/NPC-based interventions, clinically-relevant cell sources that address scientific, practical and ethical considerations must be extensively tested in relevant models of CNS disease. These cell types also need to be evaluated in the context of patient-relevant functional outcomes such as respiratory function. Induced pluripotent stem (iPS) cells are pluripotent cells generated from adult somatic cell types via expression of combinations of pluripotency-related factors, avoiding ethical issues of embryonic stem cells (Takahashi et al., 2007b). This technology allows for homogeneous derivation of cell types in large quantities for applications such as transplantation, potentially in an autologous fashion from the eventual recipient or from allogeneic sources (Das and Pal, 2010; Kiskinis and Eggan, 2010). Despite the promise of this approach, the iPS cell transplantation field is still in the early stages of evaluating therapeutic usefulness in relevant SCI models (Salewski et al., 2010).

Respiratory compromise is a major problem following cervical spinal cord trauma. Cervical SCI represents greater than half of all human cases, in addition to often resulting in the most severe physical and psychological debilitation (Lane et al., 2008). Respiratory compromise is the leading cause of morbidity and mortality following SCI. While a growing literature exists on respiratory function in animal models of SCI (Lane et al., 2008; Lane et al., 2009), few studies have examined cellular mechanisms involved in protection of this vital neural

circuitry, and little work has been conducted to test therapies for targeting cervical spinal cord-related functional outcome measures such as breathing. Phrenic motor neuron (PhMN) loss plays a central role in respiratory compromise following cervical SCI. The diaphragm, a major inspiratory muscle, is innervated by PhMNs located at cervical levels 3–5 (Lane et al., 2009). PhMN output is driven by descending pre-motor bulbospinal neurons in the medullary rostral ventral respiratory group (rVRG) (Zimmer et al., 2007). Cervical SCI results in diaphragmatic respiratory compromise due to PhMN loss and/or injury to descending bulbospinal respiratory axons. The majority of these injuries affect mid-cervical levels (Shanmuganathan et al., 2008) (the location of the PhMN pool), and respiratory function following mid-cervical SCI is significantly determined by PhMN loss/sparing (Strakowski et al., 2007). Although use of thoracic models has predominated, cervical SCI animal models have recently been developed (Aguilar and Steward, 2010; Awad et al., 2013; Gensel et al., 2006; Lane et al., 2012; Lee et al., 2010; Sandrow-Feinberg et al., 2009; Sandrow-Feinberg et al., 2010; Sandrow et al., 2008; Stamegna et al., 2011), including our own (Nicaise et al., 2012). Because of the relevance of astrocyte and GLT1 dysfunction to PhMN loss/injury following cervical trauma, we targeted transplantation in the present study to cervical spinal cord ventral horn in a cervical contusion SCI model.

We previously investigated the therapeutic efficacy of transplanting rodent-derived glial-restricted precursors (GRP), a class of lineage-restricted astrocyte progenitor cell (Li et al., 2014a). We transplanted either undifferentiated GRPs or GRP-derived astrocytes (pre-differentiated *in vitro* prior to injection) into our model of cervical contusion SCI, and found that both cell types survived, localized to the ventral horn and efficiently differentiated into mature astrocytes. However, animals injected with GRP-derived astrocytes had higher levels of intraspinal GLT1 expression than those injected with undifferentiated GRPs, suggesting that pre-differentiation enhanced the *in vivo* maturation of these cells. We also observed that modifying GRP-derived astrocytes to constitutively express GLT1 was more effective in achieving *in vivo* GLT1 expression and for protecting PhMNs.

Given the importance of astrocytes in SCI pathogenesis, the observations of GLT1 dysfunction following SCI, and our previous success targeting astrocyte GLT1 using rodent-derived glial progenitor cells, in the present study we evaluated intraspinal transplantation of hiPS cell-derived astrocytes (hIPSA) into ventral horn following cervical contusion SCI as a novel therapeutic strategy for reconstituting GLT1 function. Specifically, we examined the *in vivo* fate of hIPSA transplants in the injured spinal cord of both mouse and rat models of cervical contusion SCI, including long-term survival and integration, astrocyte differentiation, maturation into GLT1-expressing cells and safety. We also tested the therapeutic efficacy of hIPSA transplantation for protection of PhMNs and preservation of diaphragm function.

Derivation of cell types from iPS cells represents a relevant approach for clinical translation; therefore, it is critical to test both the safety and efficacy of these transplants in a patient-relevant SCI model. Importantly, previous work has shown that human- and rodent-derived versions of a given stem/progenitor type do not necessarily show similar *in vivo* fate or therapeutic properties in the disease nervous system. For example, we previously demonstrated that, following transplantation into the SOD1^{G93A} rodent model of ALS,

human glial progenitors cells show more persistent proliferation, greater migratory capacity, reduced efficiency of astrocyte differentiation, and decreased GLT1 expression compared to their rodent counterparts, which resulted in a lack of therapeutic efficacy only with the human cells (Lepore et al., 2011b; Lepore et al., 2008b). It is therefore important to extend our previous studies with rodent-derived glial progenitors in the cervical contusion SCI model to now test human iPS cells.

Materials and methods

Animals

Transplantation into rats and mice—Female Sprague-Dawley rats weighing 250–300 grams were purchased from Taconic Farm (Rockville, MD). Female C57BL/6 wild-type mice weighing 20–30 grams were purchased from The Jackson Laboratory (Bar Harbor, ME). All animals were housed in a humidity-, temperature-, and light-controlled animal facility with *ad libitum* access to water and food. Experimental procedures were approved by the Thomas Jefferson University IACUC and conducted in compliance with ARRIVE (*Animal Research: Reporting of In Vivo Experiments*) guidelines.

Cervical contusion SCI

Rat SCI—Rats were anesthetized with ketamine (100 mg/kg), xylazine (5 mg/kg) and acepromazine (2 mg/kg). The cervical dorsal skin and underlying muscles were incised. The paravertebral muscles overlying C3–C5 were removed. Following unilateral laminectomy on the right side at C3, C4 and C5 levels, rats were subjected to a C4 spinal contusion injury with the Infinite Horizon impactor (Precision Systems and Instrumentation, Lexington, KY) using a 1.5mm tip at a force of 395 kDynes. This injury paradigm is based on our previously published rat model that results in robust PhMN degeneration and chronic diaphragm dysfunction (Nicaise et al., 2013; Nicaise et al., 2012). Rats were transplanted in all studies immediately following injury. After surgical procedures, overlying muscles were closed in layers with sterile 4-0 silk sutures, and the skin incision was closed using wound clips. Animals were allowed to recover on a circulating warm water heating pad until awake and then returned to their home cages. They were monitored daily until sacrifice, and measures were taken to avoid dehydration and to minimize any pain or discomfort.

Mouse SCI—Mice were anesthetized with a cocktail of ketamine (120 mg/kg) and xylazine (5 mg/kg). The surgical procedure and post-surgical monitoring used for mice were the same as described above for rats. For the contusion injury, the 1mm impactor tip was raised 1.25mm above the dura prior to impact, and a force of 50 kDynes (kD) was used for impact.

Virus production

Lentiviral vector carrying the green fluorescent protein (GFP) gene or GLT1 gene was packaged in 293FT cells. Briefly, To produce control lentiviral-GFP vector, 293FT cells were transfected with pCDH-MSCV-MCS-EF1-GFP plasmid (System Biosciences, Mountain View, CA) and three other helper plasmids, pLP-1, pLP-2, and pLP/VSVG with Polyfect (Qiagen, Valencia, CA). To produce lentiviral-GLT1 vector, GLT1 gene CDS

fragment was inserted into MCS of pCDH-MSCV-MCS-EF1-GFP plasmid, and the vector plasmid was then transfected into 293FT cells with three helper plasmids as described above. Supernatant was collected 72 hours later, and lentiviral vector was concentrated with PEG-it Virus Precipitation Solution (System Biosciences, Mountain View, CA) and re-suspended with PBS to the final titer of 1×10^8 infectious units/ml.

Human induced pluripotent stem cell derived astrocytes

Human iPS cell derivation, culturing and astrocyte differentiation—iPS cells were derived from non-diseased healthy patient donors. Dermal fibroblasts were reprogrammed into iPS cells via retroviral transduction with KLF4, SOX2, OCT4, and c-MYC (Takahashi et al., 2007a). By immunohistochemistry and qRT-PCR, these putative iPS cells expressed proteins and transcripts associated with pluripotency, including Sox 2, and stem cell-associated antigens, including SSEA4, Nanog, alkaline phosphatase, and TRA 1–81, and capacity to differentiate into cells of three germ layers was established. Finally, the karyotype of these iPS cells was found to be normal. Once pluripotent iPS cells were generated, the stem cells were cultured in E8 medium (Life Technologies, Grand Island, NY). To maintain optimum pluripotency and limit spontaneous differentiation, the stem cell colonies were manually cleaned once every 6 days just before passage using dispase (Stem Cell Technologies, Vancouver, BC). To differentiate the iPS cells into astrocytes, a protocol previously described by Haidet-Phillips and colleagues (Haidet-Phillips et al., 2014) was used. To summarize, iPS cells were lifted with dispase, gently separated into single cells and plated as a monolayer. Using the smad dual inhibition pathway method to direct differentiation toward a neural phenotype, the cells were incubated in DMEM/F12 (Life Technologies, Grand Island, NY) enriched with $0.2 \mu\text{M}$ LDN (Stemgent, Cambridge, MA) and $10 \mu\text{M}$ SB431542 (Sigma, Saint Louis, MO). The cells were then exposed to $1 \mu\text{M}$ retinoic acid (Sigma, Saint Louis MO) and N2 (Life Technologies, Grand Island, NY) starting at day 5 and Sonic HedgeHog (Life Technologies, Grand Island, NY) starting at day 8. From day 15 to day 30 after starting the differentiation protocol, the medium was gradually changed to neurobasal medium. After day 30, to differentiate these iPS cell-derived glial progenitors into astrocytes, cells were maintained and expanded in DMEM/F12 supplemented with 1% Fetal Bovine Serum, B27, L-glutamine, non-essential amino acids, penicillin/streptomycin (all from Life Technologies, Grand Island, NY) and $2 \mu\text{g/ml}$ Heparin (Sigma-Aldrich, St. Louis, MO) for an additional 60 days. Astrocytes derived from human iPS were identified with immunostaining using GFAP antibody. For feeding and passaging of astrocyte progenitor cultures, cells were rinsed with PBS and incubated with 4 ml of 0.05% trypsin for 5 minutes. Cells were collected in trypsin and rinsed with 7 ml of culture medium and $1 \times$ trypsin inhibitor (Life Technologies, Grand Island, NY) to stop trypsinization. Cells were centrifuged at 1000 rpm for 5 minutes and re-suspended in fresh culture medium. Cells were counted and seeded onto poly-L-lysine coated dishes. Cells were fed twice a week and were passaged after they were 80%–90% confluent.

GLT1 overexpression—After differentiation for 90 days, hIPSA (astrocytes derived from human iPS cells) were transduced with lentiviral-GFP vector or lentiviral-GLT1 vector, at the concentration of 1×10^6 infectious units/ml, one week before transplantation.

On the second day of transduction, culture medium was changed and the cells were cultured for 5 more days.

Human dermal fibroblasts

Human dermal fibroblast cells (ATCC, Manassas, VA) were cultured with Fibroblast Growth Kit-low serum (ATCC, Manassas, VA). Fibroblasts were transduced with control lentiviral-GFP vector one week before transplantation. Transduced GFP was used to track transplanted cells *in vivo*.

Transplantation

Cell preparation for transplantation—On the day of transplantation, cells were rinsed with PBS and trypsinized with 0.05% trypsin, collected and rinsed with culture medium and 1× trypsin inhibitor. The cells were washed with artificial cerebrospinal fluid twice. Cell viability was assessed using the trypan blue assay and was always found to be greater than 80%. The final cell concentration was adjusted to 1×10^8 cells/ml.

Intraspinal transplantation—Transplantation was conducted on deeply anesthetized rats and mice immediately post-injury. Following unilateral right-sided contusion injury at C4, cells were injected into the spinal cord at two locations. Each site contained 2µL of cell suspension, which was administered into the spinal cord ventral horn using a Hamilton gas-tight syringe mounted on an electronic UMP3 micropump (World Precision International, Sarasota, FL) (Lepore and Maragakis, 2011; Lepore et al., 2011a). The sites of injections were located at the rostral and caudal edges of the contusion site. Ventral horns were targeted by lowering the 33-gauge 45-degree beveled needle 1.5mm below the dorsal surface of the spinal cord. Each injection was delivered at a constant rate over 5 minutes. Upon completion of cell delivery, overlying muscles were then closed in layers with sterile 4-0 silk sutures, and the skin incision was closed using sterile wound clips. Animals were allowed to recover and monitored daily.

Immune suppression—All animals were immune suppressed. Rats received subcutaneous administration of cyclosporine A (10mg/kg; Sandoz Pharmaceuticals, East Hanover, NJ) daily beginning three days before grafting and continuously until sacrifice. Mice were given both FK-506 and rapamycin (1 mg/kg each; LC Laboratories; Woburn, MA).

Tissue processing for histology

At the time of sacrifice, animals were anesthetized, and diaphragm muscle was freshly removed prior to perfusion and then further processed for neuromuscular junction (NMJ) labeling. Animals were transcardially perfused with 0.9% saline, followed by 4% paraformaldehyde infusion. Spinal cords were harvested, then cryoprotected in 30% sucrose for 3 days and embedded in freezing medium. Spinal cord tissue blocks were cut serially in the sagittal or transverse planes at a thickness of 30µm. Sections were collected on glass slides and stored at -20°C until analysis. Spinal cord sections were thawed, allowed to dry for 1 hour at room temperature, and stained with 0.5% Cresyl violet acetate according to standard procedure (Nicaise et al., 2012).

Immunohistochemistry

Frozen spinal cord sections were air-dried, washed with PBS, permeabilized with 0.4% Triton X-100 in PBS for 5 minutes at room temperature, and then incubated in blocking solution (PBS containing 10% normal goat serum and 0.4% Triton X-100) for 1 hour at room temperature. Sections were labeled overnight at 4°C with the primary antibodies in blocking solution. Sections were then washed three times with PBS (5 minutes per wash) and incubated with secondary antibodies in blocking solution for 1 hour at room temperature. After washing twice with PBS (10 minutes per wash), sections were cover-slipped. A number of primary antibodies were used. Mouse anti-GFAP antibody (EMD Millipore Corporation, Billerica, MA; 1:200) and rabbit anti-GFAP antibody (Dako North America, Carpinteria, CA; 1:200) were used to label astrocytes (Lepore et al., 2008a). Mouse anti-human GFAP antibody (StemCells, Inc, Newark, CA; 1:200) was used to label astrocytes of human origin in mice and rats. Rabbit anti-GLT1 (1:800) and mouse anti-GLT1 (1:200) were used to label GLT1 protein (both were provided by Jeffrey Rothstein's laboratory) (Lepore et al., 2008b). Rabbit anti-Ki67 (Thermo Fisher Scientific, Rockford, IL; 1:200) labeled proliferating cells (Lepore et al., 2008a). Mouse anti-human cytoplasmic marker antibody (StemCells, Inc, Newark, CA; 1:200) and mouse anti-HuNu antibody (EMD Millipore Corporation, Billerica, MA; 1:200) were used to label human cytoplasm and human nuclear antigen, respectively, for selectively identifying human-derived cells. Secondary antibodies included: FITC goat-anti-mouse IgG, FITC goat-anti-rabbit IgG, TRITC goat-anti-mouse IgG, TRITC goat-anti-rabbit IgG, Alexa Fluor 647 goat-anti-mouse IgG, Alexa Fluor 647 goat-anti-rabbit IgG. All secondary antibodies (Jackson ImmunoResearch Laboratories, West Grove, PA) were diluted at 1:200 to recognize the matched primary antibody. For fluorescence analysis, sections were cover-slipped with fluorescent-compatible mounting medium (ProLong Gold, Life Technologies, Grand Island, NY).

Quantification of in vitro cultured cell differentiation, proliferation and GLT1 expression

The proportions of GFAP⁺ astrocytes and Ki67⁺ proliferating cells were expressed as a percentage of the total number of cultured cells (labeled by DAPI). In order to quantify double-labeling of DAPI with GFAP or Ki67, images were taken at 10× magnification and analyzed using ImageJ software. In each image, cells with a DAPI⁺ nucleus were assessed for expression of GFAP or Ki67.

Quantification of transplant differentiation

Rats and mice were sacrificed for quantification of astrocyte differentiation (GFAP⁺) and proliferation (Ki67⁺). The proportions GFAP⁺ astrocytes and Ki67⁺ proliferating cells were expressed as a percentage of the total number of transplanted human cells (labeled by anti-hCytoplasm or HuNu antibody). In order to quantify double-labeling of hCytoplasm or HuNA with GFAP and Ki67, double-labeled transverse sections were imaged at 10× magnification using MetaMorph software and were then analyzed using ImageJ software. In each image, cells expressing hCytoplasm or HuNu were assessed for co-expression of GFAP or Ki67.

Quantification of GLT1 expression by transplants

Rats and mice were sacrificed for quantification of GLT1 expression by hCyto-labeled cells in the ventral horn. GLT1⁺ and hCyto⁺ cells were identified in the ventral horn using ImageJ software, and the percentage of hCyto⁺ cells (representing any transplant-derived cell) that co-expressed GLT1 were quantified.

Lesion imaging and quantification

Images were acquired with a Zeiss Imager M2 upright microscope and analyzed with ImageJ software. Lesion size was quantified in Cresyl violet stained sections (Li et al., 2014b). Specifically, lesion area was determined in every 10th section by tracing both the total area of the hemi-spinal cord ipsilateral to the contusion site and the actual lesion area. Lesion was defined as areas including both lost tissue (cystic cavity formation) and surrounding damaged tissue in which the normal anatomical structure of the spinal cord was lost. The lesion epicenter was defined as the section with the largest percent lesioned tissue (relative to total tissue area in the same section).

Neuromuscular junction (NMJ) analysis

Fresh hemi-diaphragm muscle was dissected from each animal for whole-mount immunohistochemistry, as described previously (Wright et al., 2007). Hemi-diaphragm muscle was dissected, stretched, pinned down to Sylgard medium (Fisher Scientific, Pittsburgh, PA), and extensively cleaned to remove any connective tissue to allow for antibody penetration. Motor axons and their terminals were labeled with SMI-312R (Covance, Princeton, NJ; 1:1000) and SV2-s (DSHB, Iowa City, IA; 1:10), respectively, and both primary antibodies were detected with FITC anti-mouse IgG secondary (Jackson ImmunoResearch Laboratories, West Grove, PA; 1:100). Post-synaptic acetylcholine receptors were labeled with rhodamine-conjugated alpha-bungarotoxin (Life Technologies, Grand Island, NY; 1:400). Labeled muscles were analyzed for total numbers of NMJs and intact, denervated and multiply-innervated NMJs. Whole-mounted diaphragms were imaged on a FluoView FV1000 confocal microscope (Olympus, Center Valley, PA). We only conducted NMJ analysis in ipsilateral hemi-diaphragm because in our previously published work we did not observe denervation or sprouting in contralateral hemi-diaphragm after cervical hemi-contusion SCI (Nicaise et al., 2012).

Functional glutamate uptake assay

After transduction with lentiviral-GFP vector or lentiviral-GLT1 vector, hIPSAs were cultured for 10 days. Human fibroblasts transduced with lentiviral-GFP vector were used as control. Glutamate uptake activity was measured as previously described (Dowd and Robinson, 1996), with slight modification. Briefly, cells were washed and pre-incubated with either a sodium- or choline-containing uptake buffer (in mM: Tris, 5; HEPES, 10; NaCl or choline chloride, 140; KCl, 2.5; CaCl₂, 1.2; MgCl₂, 1.2; K₂HPO₄, 1.2; glucose, 10) for 20 min at 37°C; and in DHK treatment groups, 100µM of DHK was added to inhibit GLT1. The uptake buffer was then replaced with fresh uptake buffer containing 20nM ³H-glutamate (49 Ci/mmol; PerkinElmer, CA) and 20µM unlabeled glutamate. The cells were incubated for 5 minutes at 37°C. The reaction was terminated by washing cells three times

with choline-containing uptake buffer containing 2mM unlabeled glutamate, followed by immediate lysis in ice-cold 0.1N NaOH. Cell extracts were then measured with a liquid scintillation counter (Beckman Instruments, Fullerton, CA). The protein content in each well was measured using the Bradford protein assay (Bio-Rad, Hercules, CA).

Diaphragm Compound Muscle Action Potentials (CMAPs)

Rats were anesthetized in the same manner described above. Phrenic nerve conduction studies were performed with single stimulation (0.5 ms duration; 6 mV amplitude) at the neck via near nerve needle electrodes placed along the phrenic nerve (Li et al., 2014b; Nicaise et al., 2012). The ground needle electrode was placed in the tail, and the reference electrode was placed subcutaneously in the right abdominal region. Recording was obtained via a surface strip along the costal margin of the diaphragm, and CMAP amplitude was measured baseline to peak. Recordings were made using an ADI Powerlab 8/30 stimulator and BioAMP amplifier (ADInstruments, Colorado Springs, CO), followed by computer-assisted data analysis (Scope 3.5.6, ADInstruments). For each animal, 10–20 tracings were averaged to ensure reproducibility.

Spontaneous EMG recordings

Prior to being euthanized, animals received a laparotomy. These EMG recordings were terminal experiments and were only conducted immediately prior to euthanasia. Bipolar electrodes spaced by 3 mm were inserted into specific subregions of the right hemidiaphragm (i.e. dorsal, medial or ventral regions) (Li et al., 2014b). Activity was recorded and averaged during spontaneous breathing at each of these 3 locations separately in each animal. The EMG signal was amplified, filtered through a band-pass filter (50–3000 Hz), and integrated using LabChart 7 software (ADInstruments). Parameters such as inspiratory bursts per minute, discharge duration and integrated peak amplitude were averaged over 2 minute sample periods. No attempt was made to control or monitor the overall level of respiratory motor drive during the EMG recordings.

Statistics

Results were expressed as means \pm standard error of the mean (SEM). A Kolmogorov–Smirnov test was conducted for all variables to assess normality. Unpaired *t* test or Mann-Whitney was used to assess statistical significance between two groups. With respect to multiple comparisons involving three groups or more, statistical significance was assessed by analysis of variance (one-way ANOVA) followed by post-hoc test (Bonferroni's method). Statistics were computed with Graphpad Prism 5 (GraphPad Software, Inc., La Jolla, CA). $p < 0.05$ was considered as statistically significant.

Results

***In vitro* characterization of human iPS cell-derived astrocytes (hIPSAs)**

We differentiated human iPS cells into astrocytes by culturing them in differentiating medium containing FBS. We transduced cells with lentivirus (LV)-GFP or LV-GLT1-GFP to generate control cells (GFP-hIPSAs) and GLT1-overexpressing hIPSAs (GLT1-hIPSAs), respectively. The GFP-hIPSAs expressed little-to-no GLT1 protein (Fig. 1A, C), consistent

with the limited expression of GLT1 by cultured astrocytes in the absence of neuronal co-culture (Li et al., 2014a; Perego et al., 2000), while GLT1-hiPSAs expressed high levels of GLT1 protein *in vitro* (Fig. 1B, C). In addition, the vast majority of DAPI⁺ GLT1-hiPSAs expressed GLT1 (Fig. 1B), which is expected given the high efficiency of transduction with our lentivirus (not shown). GLT1 overexpression did not alter hiPSA differentiation (Fig. 1D, E, H) or proliferation (Fig. 1F–H). In addition to significantly increased GLT1 protein expression levels, GLT1-hiPSAs showed a large increase in functional GLT1-mediated glutamate uptake compared to GFP-hiPSAs using an *in vitro* ³H-glutamate uptake assay (Fig. 1J). In this ³H-glutamate uptake assay and in the subsequent transplantation experiments, we used LV-GFP transduced human fibroblasts (GFP-hFibro) (Fig. 1I) as a non-glia cell control.

Human iPSA transplants robustly survived and differentiated into astrocytes following rat cervical contusion SCI

We characterized the fate of transplanted hiPSAs in both rats and mice following unilateral C4 contusion SCI, given the usefulness of both experimental models for studying nervous system diseases. Immediately following injury, we injected hiPSAs directly into the ventral horn at locations just rostral and caudal to the contusion site (Fig. 2A). We specifically delivered cells into the ventral horn to anatomically target the location of the PhMN pool (Fig. 2B).

We sacrificed rats at 2 days, 2 weeks and 4 weeks post-injury/transplantation. Double-labeling with panGFAP antibody and a human-specific GFAP antibody demonstrated that transplanted human-derived cells differentiated into astrocytes (Fig. 2C). Both transplanted GFP-hiPSAs (Fig. 2D, F, H) and GLT1-hiPSAs (Fig. 2E, G, I) robustly survived out to W4, and nearly all hCytoplasm⁺ transplant-derived cells co-labeled with the astrocyte lineage marker, GFAP, at D2 (Fig. 2D–E), W2 (Fig. F–G) and W4 (Fig. 2H–I). There were no differences in the degree of astrocyte differentiation between GFP-hiPSAs and GLT1-hiPSAs at any of these time points (quantification shown in Fig. 2J). LV-GFP transduced human fibroblasts (GFP-hFibro) also survived in the injured spinal cord to at least W4 post-injury (Fig. 2K).

Despite efficient astrocyte differentiation, only a small percentage of GFP-hiPSA transplant-derived cells expressed GLT1 protein in the injury site at D2 (Fig. 3A), W2 (Fig. 3C) and W4 (Fig. 3E). On the contrary, the majority of GLT1-hiPSAs robustly expressed GLT1 at all times (Fig. 3B, D, and F) (quantification: Fig. 3G).

Human iPSA transplants showed limited proliferation *in vivo* and did not form tumors

A major concern regarding NSC/NPC therapy (particularly with pluripotent cells such as iPS cells) is the potential for uncontrolled proliferation and even tumor formation. To address this concern, we immunostained for the proliferation marker, Ki67, and we examined transplant recipient rat spinal cords for overt tumor formation. With both GFP-hiPSAs (Fig. 4A, C, E) and GLT1-hiPSAs (Fig. 4B, D, F), less than 10% of HuNu⁺ transplant-derived cells expressed Ki67 at D2 (Fig. 4A–B), W2 (Fig. 4C–D) and W4 (Fig.

4E–F) (quantification shown in Fig. 4G). In addition, we never observed tumor formation in any transplant-recipient animals.

Human iPSA transplants showed similar survival and differentiation in the injured mouse cervical spinal cord

Given the usefulness of the mouse model due to the availability of transgenic tools, we conducted similar characterization of hIPSA fate following transplantation into the mouse spinal cord immediately following unilateral cervical contusion SCI. Similar to transplantation into the rat SCI model, hIPSAs robustly survived and integrated for at least 4 weeks post-injection. The majority of transplant-derived cells were differentiated GFAP⁺ astrocytes (Fig. 4H). Control GFP-hIPSAs expressed little GLUT1, while overexpression resulted in the majority of transplant-derived astrocytes expressing GLUT1 (Fig. 4I). Less than 10% of transplant-derived cells continued to proliferate at D2, W2 and W4 (Fig. 4J), and again we never observed tumor formation in any mice.

GLT1 overexpressing hIPSA transplants reduced lesion size following cervical contusion SCI

To test the therapeutic efficacy of hIPSA transplants in the rat unilateral cervical contusion model, we first assessed lesion size. At 4 weeks post-injury, we quantified Cresyl-violet stained transverse sections of the cervical spinal cord surrounding the injury site for the degree of ipsilesional tissue sparing by calculating the percentage of total ipsilateral hemi-cord area comprised of damaged tissue (Fig. 5A). Lesion area (Fig. 5B) and total lesion volume (Fig. 5C) analysis (combined for both white and gray matter) revealed that GLUT1-hIPSA transplants significantly reduced lesion size at multiple locations surrounding the epicenter compared to both GFP-hFibro and GFP-hIPSA control transplant groups. We observed this protective effect specifically within 1mm rostral and caudal of the epicenter where the greatest tissue damage occurred.

GLT1 overexpressing hIPSA transplants preserved diaphragm innervation by phrenic motor neurons after SCI

We found that GLUT1 overexpressing hIPSA transplants significantly preserved morphological innervation at the diaphragm neuromuscular junction (NMJ), the synapse which is critical for functional PMN-diaphragm connectivity. To examine pathological alterations at the diaphragm NMJ, we analyzed hemi-diaphragm muscle ipsilateral to the contusion in rats (Fig. 6A–B). We quantified the percentage of intact NMJs or partially denervated NMJs in the animals from the 3 injection groups at 4 weeks post-injury/transplantation (Wright et al., 2007; Wright et al., 2009; Wright and Son, 2007). For analysis, we divided the hemi-diaphragm into three anatomical regions (ventral, medial and dorsal) (Fig. 6C), as the rostral-caudal axis of the PMN pool within the cervical spinal cord topographically maps onto the ventral-dorsal axis of the diaphragm (Laskowski and Sanes, 1987). At the dorsal region of the hemi-diaphragm, the percentage of intact NMJs in the GLUT1-hIPSA transplant group was significantly greater than both control groups, while at the ventral and medial regions of the diaphragm, there were no differences in the percentage of intact NMJs amongst the groups (Fig. 6D). GLUT1-hIPSA transplants also significantly

reduced the percentage of partially denervated NMJs in the medial and dorsal hemi-diaphragm regions compared to both control groups (Fig. 6E).

GLT1 overexpressing hIPSA transplants preserved diaphragm function following cervical contusion SCI

To determine the efficacy of preserving PMN-diaphragm innervation with respect to respiratory impairment, we characterized the *in vivo* functional effects of transplants on diaphragmatic function in cervical contusion rats. We recorded spontaneous EMG activity, which is indicative of PMN activation of diaphragm muscle due to central drive, at 4 weeks post-injury/transplantation (Fig. 7A). All groups showed reduced amplitude in rhythmic inspiratory EMG bursts associated with muscle contraction compared to uninjured animals (Nicaise et al., 2012). Integrated EMG analysis of this recording shows that the GLT1-hIPSA transplants significantly increased EMG amplitude in the dorsal region of the hemi-diaphragm compared to both control groups (Fig. 7B), again matching the anatomically-specific spinal cord and NMJ histological results. However, we observed no protective effects of GLT1-hIPSA transplants at either the medial or ventral regions, and the control GFP-hIPSA transplants showed no significant effects compared to control hFibroblast injection at all hemi-diaphragm locations (Fig. 7B). There were no significant differences in EMG burst frequency (Fig. 7C) or burst duration (Fig. 7D) amongst the three groups.

Following supramaximal phrenic nerve stimulus, we obtained compound muscle action potentials (CMAP) recordings from the ipsilateral hemi-diaphragm using a surface electrode (Fig. 7E). In all treatment groups, peak CMAP amplitude was significantly reduced compared to uninjured laminectomy only rats, whose CMAP amplitudes are approximately 7mV (Nicaise et al., 2013). However, CMAP amplitudes in the GLT1-hIPSAtransplant group were significantly increased compared to the two control transplantation groups at weeks 2–4 post-injury (Fig. 7F). With the use of the surface electrode, we are recording from the entire hemi-diaphragm (or at least a significant portion of the muscle), yet we still observed this significant protective effect on overall muscle function, despite the fact that transplants only reduced central degeneration very near to the injury site and correspondingly preserved morphological innervation only in the dorsal hemi-diaphragm.

Discussion

The use of iPS cells as a source of mature cell types for therapeutic transplantation in CNS diseases represents an exciting direction in regenerative medicine. However, to date only a small number of studies have assessed the long-term fate and therapeutic efficacy of iPS cell-derived transplants in animal models of SCI.

A number of these studies reported significant therapeutic benefit when NSCs/NPCs derived from either mouse (Tsuji et al., 2010) or human (Fujimoto et al., 2012; Nori et al., 2011; Romanyuk et al., 2014) iPS cells were transplanted into contusion or cavity-type models of rodent SCI, as well as in non-human primate models (Kobayashi et al., 2012). Unlike our current work, these studies did not focus on, or achieve, targeted replacement of astrocytes in the injured spinal cord. In many cases, the cells were delivered in a multipotent NSC-like state and resulted in mixed differentiation into glial phenotypes, including astrocytes, and

various neuronal subtypes. While these studies were able to achieve some functional benefit, future work may require more phenotypically targeted strategies, each of which depends on the nature of the SCI pathology (e.g. type of injury, anatomical locations affected, etc.) and the specific cell lineages being targeted for replacement. Nevertheless, these studies were able to nicely show promising properties of engrafted cells in the injured spinal cord environment, including synaptic integration into endogenous neuronal circuitry (Fujimoto et al., 2012; Nori et al., 2011). iPS cell-derived NSCs have also shown therapeutic promise in models of other spinal cord diseases such as spinal muscular atrophy (Simone et al., 2014).

A number of these studies with iPS cell transplantation reported a lack of beneficial outcomes in SCI models. Pomeshchik and colleagues (Pomeshchik et al., 2014) did not observe functional improvement after transplantation of hIPS cell-derived NPCs in a contusion SCI model. However, they also did not find long term survival of grafted cells in these mice receiving a tacrolimus immune suppression regimen, unlike the robust and persistent integration that we observed in the present study using an immune suppression protocol consisting of both tacrolimus and rapamycin in mice or cyclosporine in rats. In addition to our work, other groups have reported impressive survival and differentiation of hIPS cells into mature CNS cell types after injection into adult spinal cord of similarly immunosuppressed rodents (Haidet-Phillips et al., 2014; Sareen et al., 2014).

An interesting study from the Horner group (Nutt et al., 2013) reported a lack of therapeutic improvement with transplantation of hIPS cell-derived NPCs in a SCI model, despite impressive graft integration. However, cells were delivered at a chronic time point, which may represent an environment less amenable to transplant-induced plasticity, while we targeted early neuroprotection in this report.

A recent study from the Steward lab reported that transplantation of a mixed population of glial and neuronal progenitors into a transection model of SCI resulted in ectopic engraftment of large numbers of graft-derived cells in locations such as the central canal, ventricles and pial surface of the spinal cord (Steward et al., 2014), providing a note of caution when using transplantation of any class of NSC/NPC in SCI. This issue is particularly relevant to strategies employing cells derived from pluripotent sources such as ES and iPS cells given the possibility of incomplete and/or inefficient differentiation (Tsuji et al., 2010). In the current study and in our previous work (Lepore et al., 2005; Lepore and Fischer, 2005; Lepore et al., 2004; Lepore et al., 2006; Lepore et al., 2011b; Lepore et al., 2008b; Li et al., 2014a), we never observed overt tumor formation or extensive migration away from injection sites beyond only a few spinal segments. In the current work, we did note the presence of a small residual population of proliferating transplant-derived cells even out to four weeks post-injection, though we never found any tumor formation. It will be important to assess very long-term time points post-transplantation in future experiments to establish the safety of these and similar types of cells before proceeding to the clinic. Unlike the Steward paper, we did not systematically assess distribution of transplant-derived cells throughout the neuraxis.

Mechanical allodynia (a form of neuropathic pain) was observed when mouse iPAs were transplanted into a contusion SCI model (Hayashi et al., 2011). In addition to this work,

other published studies have similarly reported sensory hypersensitivity in SCI models accompanying transplantation of progenitor-derived astrocytes (Davies et al., 2008; Hofstetter et al., 2005), possibly due to increased neuronal plasticity that is induced by transplantation of immature astrocyte populations (Smith et al., 1986). However, in a large body of work, we and others (Haas et al., 2012; Mitsui et al., 2005; Nutt et al., 2013) have not found such increased sensitivity, including following hIPSA transplantation (Nutt et al., 2013). The discrepancy amongst these studies may be due to heterogeneity in the subtypes of astrocytes being injected (Davies et al., 2008; Davies et al., 2011).

A number of practical issues that are beyond the scope of this discussion will need to be addressed before moving transplantation of iPS cells to the clinic in SCI and other diseases of the nervous system. Specifically with respect to targeting relative early events such as PhMN loss after cervical SCI, autologous derivation of cells will likely not be relevant given that PhMNs are lost within several days post-injury (Nicaise et al., 2013). Instead, cells to be used for transplantation will likely be obtained from banks of immune/HLA-matched cells (Zimmermann et al., 2012). Given the need to extensively test iPS cell lines prior to transplantation into a patient, as well as the costs and time that will be required for generating cells for each individual patient, this approach may actually be practically preferable to autologous derivation (Taylor et al., 2011). As human stem cell lines have shown donor variability in SCI models (Neuhuber et al., 2005), future studies will need to investigate *in vivo* properties and therapeutic efficacy of human iPS cells derived from multiple donors in an attempt to move this approach towards clinical translation.

Similar to our previous work using transplantation of astrocytes derived from rodent glial progenitors (Li et al., 2014a), we find that GLT1-overexpressing hIPSA promote significant preservation of diaphragm function and diaphragm innervation by PhMNs. In both studies, control unmodified transplant-derived astrocytes expressed relatively lower levels of GLT1 in the injured spinal cord, suggesting that the cells respond to the injured environment in a similar manner as host astrocytes that show extensive transporter downregulation. Interestingly, the unmodified hIPSA transplants, despite excellent survival and efficient differentiation, did not promote therapeutic benefit with respect to protection of diaphragmatic respiratory circuitry. These findings suggest that astrocyte replacement alone may insufficient when targeting certain pathological mechanisms (e.g. excitotoxicity) but that functional maturation of these astrocytes is necessary, which is not surprising given the diverse, complex and integral roles that astrocytes play in intact CNS function (Pekny and Nilsson, 2005).

We have made interesting observations over the course of a number of studies with respect to therapeutically targeting GLT1 following SCI. We have consistently observed significant GLT1 downregulation in endogenous reactive astrocyte populations in both contusion and crush, as well as both cervical and thoracic, models of SCI (Lepore et al., 2011a; Lepore et al., 2011c; Li et al., 2014b; Putatunda et al., 2014; Watson et al., 2014). When we selectively increased GLT1 expression in these endogenous astrocytes in the unilateral cervical contusion model using an AAV8 vector, we paradoxically found that secondary degeneration of PhMNs and diaphragm denervation were worsened (Li et al., 2014b). This effect was due to compromise in the protective glial scar-forming properties of endogenous

astrocytes, which resulted in unexpected expansion of the lesion. In the current study with hIPSAs and in our previous work with rodent-derived glial progenitors (Li et al., 2014a), we found that delivery of an exogenous source of astrocytes that expresses high levels of functional GLT1 via transplantation (in the exact same cervical contusion model) results in significant preservation of PhMNs and diaphragm function. These findings, as well as other studies that tested the effects of pharmacologically elevating (Olsen et al., 2010) or genetically reducing (Lepore et al., 2011c) GLT1 in SCI, demonstrate that targeting GLT1 is a promising and powerful therapeutic strategy in SCI for targeting neuroprotection and possibly other outcomes of SCI such as neuronal hyperexcitability.

Despite the impressive therapeutic effect achieved in the present study, the degree of PhMN protection and diaphragm function preservation was only partial. In future work, we will need to optimize neuroprotective strategies such as hIPSA transplantation to enhance therapeutic effects, as well as combine these neuroprotective approaches with interventions aimed at promoting plasticity, axonal regrowth and targeted reconnection of the rVRG-PhMN-diaphragm circuit (Alilain et al., 2011). Preserving neural control of diaphragm function involves targeting a complex circuitry that extends beyond just protecting PhMNs (Lane et al., 2009). We focused on preservation of PhMNs centrally in the cervical spinal cord and NMJ innervation peripherally in the diaphragm. Nevertheless, our hIPSA intervention may have also exerted beneficial effects via protection of respiratory interneuron populations of the cervical spinal cord and/or descending bulbospinal input to PhMNs from the rVRG. hIPSA transplants may have also resulted in beneficial effects by promoting regrowth/regeneration and/or sprouting of rVRG axons and interneurons, which is possible given the growth-promoting properties of astrocyte transplants after SCI (Davies et al., 2006; Davies et al., 2008; Davies et al., 2011; Haas et al., 2012). However, we only observed therapeutic effects on diaphragm innervation and function with GLT1 overexpressing hIPSA (but not with control unmodified hIPSA), suggesting that neuroprotection mediated by increased GLT1 levels and consequent reduction in excitotoxicity was the likely mechanism, even if transplants also promoted some regrowth of respiratory axon populations. We also did not observe differences amongst groups in plasticity at the diaphragm NMJ such as sprouting or reinnervation, further supporting central neuroprotection as the responsible mechanism of therapeutic action.

In conclusion, we report exciting and novel results showing that targeted replacement of astrocyte GLT1 following cervical SCI using hIPSA transplantation significantly preserves diaphragmatic respiratory function. These findings are important for a number of reasons. We demonstrate the therapeutic efficacy and safety of hiPS transplantation in SCI, as well as the benefit of specifically addressing astrocyte dysfunction using this clinically-relevant source of cells. We also show mechanistically that targeting GLT1 using an astrocyte transplant-based approach has profound effects on functional and histopathological outcomes after SCI. Furthermore, we conducted these studies in a clinically-relevant SCI paradigm that models a large proportion of human disease cases. Excitingly, we find that this intervention results in therapeutic benefit on respiratory function, which has important implications for SCI patients. Collectively, these studies lay the foundation for translating iPS cell transplantation to the treatment of SCI.

Acknowledgements

Funding

This work was supported by the Craig H. Neilsen Foundation (grant #190140 to A.C.L.) and the NINDS (grant #1R01NS079702 to A.C.L.).

Abbreviations

SCI	spinal cord injury
iPS cells	induced Pluripotent Stem cells
hIPSA	human induced Pluripotent Stem cell-derived astrocytes
GLT1	glutamate transporter 1
PhMN	phrenic motor neuron
C3 (4, 5, etc.)	cervical spinal cord level 3 (4, 5, etc.)
GRP	glial-restricted precursor
CMAP	compound muscle action potential
NMJ	neuromuscular junction
GFP-hIPSA	lentivirus-GFP transduced hIPSA
GLT1-hIPSA	lentivirus-GLT1 transduced hIPSA
GFP-hFibro	lentivirus-GFP transduced human fibroblast
LV-GFP	lentivirus-GFP
LV-GLT1	lentivirus-GLT1

References

- Aguilar RM, Steward O. A bilateral cervical contusion injury model in mice: assessment of gripping strength as a measure of forelimb motor function. *Experimental neurology*. 2010; 221:38–53. [PubMed: 19815010]
- Alilain WJ, Horn KP, Hu H, Dick TE, Silver J. Functional regeneration of respiratory pathways after spinal cord injury. *Nature*. 2011; 475:196–200. [PubMed: 21753849]
- Awad BI, Warren PM, Steinmetz MP, Alilain WJ. The role of the crossed phrenic pathway after cervical contusion injury and a new model to evaluate therapeutic interventions. *Experimental neurology*. 2013; 248:398–405.
- Das AK, Pal R. Induced pluripotent stem cells (iPSCs): the emergence of a new champion in stem cell technology-driven biomedical applications. *J Tissue Eng Regen Med*. 2010; 4:413–421.
- Davies JE, Huang C, Proschel C, Noble M, Mayer-Proschel M, Davies SJ. Astrocytes derived from glial-restricted precursors promote spinal cord repair. *J Biol*. 2006; 5:7. [PubMed: 16643674]
- Davies JE, Proschel C, Zhang N, Noble M, Mayer-Proschel M, Davies SJ. Transplanted astrocytes derived from BMP- or CNTF-treated glial-restricted precursors have opposite effects on recovery and allodynia after spinal cord injury. *J Biol*. 2008; 7:24. [PubMed: 18803859]
- Davies SJ, Shih CH, Noble M, Mayer-Proschel M, Davies JE, Proschel C. Transplantation of specific human astrocytes promotes functional recovery after spinal cord injury. *PLoS One*. 2011; 6:e17328. [PubMed: 21407803]

- Dowd LA, Robinson MB. Rapid stimulation of EAAC1-mediated Na⁺-dependent L-glutamate transport activity in C6 glioma cells by phorbol ester. *J Neurochem*. 1996; 67:508–516. [PubMed: 8764574]
- Fujimoto Y, Abematsu M, Falk A, Tsujimura K, Sanosaka T, Juliandi B, Semi K, Namihira M, Komiya S, Smith A, Nakashima K. Treatment of a mouse model of spinal cord injury by transplantation of human induced pluripotent stem cell-derived long-term self-renewing neuroepithelial-like stem cells. *Stem Cells*. 2012; 30:1163–1173. [PubMed: 22419556]
- Gage FH. Mammalian neural stem cells. *Science*. 2000; 287:1433–1438. [PubMed: 10688783]
- Gensel JC, Tovar CA, Hamers FP, Deibert RJ, Beattie MS, Bresnahan JC. Behavioral and histological characterization of unilateral cervical spinal cord contusion injury in rats. *J Neurotrauma*. 2006; 23:36–54. [PubMed: 16430371]
- Gwak YS, Kang J, Unabia GC, Hulsebosch CE. Spatial and temporal activation of spinal glial cells: Role of gliopathy in central neuropathic pain following spinal cord injury in rats. *Experimental neurology*. 2012; 234:362–372. [PubMed: 22036747]
- Haas C, Neuhuber B, Yamagami T, Rao M, Fischer I. Phenotypic analysis of astrocytes derived from glial restricted precursors and their impact on axon regeneration. *Experimental neurology*. 2012; 233:717–732. [PubMed: 22101004]
- Haidet-Phillips AM, Roybon L, Gross SK, Tuteja A, Donnelly CJ, Richard JP, Ko M, Sherman A, Eggan K, Henderson CE, Maragakis NJ. Gene profiling of human induced pluripotent stem cell-derived astrocyte progenitors following spinal cord engraftment. *Stem Cells Transl Med*. 2014; 3:575–585. [PubMed: 24604284]
- Hayashi K, Hashimoto M, Koda M, Naito AT, Murata A, Okawa A, Takahashi K, Yamazaki M. Increase of sensitivity to mechanical stimulus after transplantation of murine induced pluripotent stem cell-derived astrocytes in a rat spinal cord injury model. *J Neurosurg Spine*. 2011; 15:582–593. [PubMed: 21854127]
- Hofstetter CP, Holmstrom NA, Lilja JA, Schweinhardt P, Hao J, Spenger C, Wiesenfeld-Hallin Z, Kurpad SN, Frisen J, Olson L. Allodynia limits the usefulness of intraspinal neural stem cell grafts; directed differentiation improves outcome. *Nature neuroscience*. 2005; 8:346–353. [PubMed: 15711542]
- Hulsebosch CE. Gliopathy ensures persistent inflammation and chronic pain after spinal cord injury. *Experimental neurology*. 2008; 214:6–9. [PubMed: 18708053]
- Kiskinis E, Eggan K. Progress toward the clinical application of patient-specific pluripotent stem cells. *J Clin Invest*. 2010; 120:51–59. [PubMed: 20051636]
- Kobayashi Y, Okada Y, Itakura G, Iwai H, Nishimura S, Yasuda A, Nori S, Hikishima K, Konomi T, Fujiyoshi K, Tsuji O, Toyama Y, Yamanaka S, Nakamura M, Okano H. Pre-evaluated safe human iPSC-derived neural stem cells promote functional recovery after spinal cord injury in common marmoset without tumorigenicity. *PLoS One*. 2012; 7:e52787. [PubMed: 23300777]
- Lane MA, Fuller DD, White TE, Reier PJ. Respiratory neuroplasticity and cervical spinal cord injury: translational perspectives. *Trends in neurosciences*. 2008; 31:538–547.
- Lane MA, Lee KZ, Fuller DD, Reier PJ. Spinal circuitry and respiratory recovery following spinal cord injury. *Respiratory physiology & neurobiology*. 2009; 169:123–132. [PubMed: 19698805]
- Lane MA, Lee KZ, Salazar K, O'Steen BE, Bloom DC, Fuller DD, Reier PJ. Respiratory function following bilateral mid-cervical contusion injury in the adult rat. *Experimental neurology*. 2012; 235:197–210.
- Laskowski MB, Sanes JR. Topographic mapping of motor pools onto skeletal muscles. *J Neurosci*. 1987; 7:252–260. [PubMed: 3543250]
- Lee JH, Tigchelaar S, Liu J, Stammers AM, Streijger F, Tetzlaff W, Kwon BK. Lack of neuroprotective effects of simvastatin and minocycline in a model of cervical spinal cord injury. *Experimental neurology*. 2010; 225:219–230. [PubMed: 20599974]
- Lepore AC, Bakshi A, Swanger SA, Rao MS, Fischer I. Neural precursor cells can be delivered into the injured cervical spinal cord by intrathecal injection at the lumbar cord. *Brain research*. 2005; 1045:206–216. [PubMed: 15910779]

- Lepore AC, Dejea C, Carmen J, Rauck B, Kerr DA, Sofroniew MV, Maragakis NJ. Selective ablation of proliferating astrocytes does not affect disease outcome in either acute or chronic models of motor neuron degeneration. *Experimental neurology*. 2008a; 211:423–432. [PubMed: 18410928]
- Lepore AC, Fischer I. Lineage-restricted neural precursors survive, migrate, and differentiate following transplantation into the injured adult spinal cord. *Experimental neurology*. 2005; 194:230–242. [PubMed: 15899260]
- Lepore AC, Han SS, Tyler-Polsz C, Cai J, Rao MS, Fischer I. Differential fate of multipotent and lineage-restricted neural precursors following transplantation into the adult CNS. *Neuron Glia Biology*. 2004; 1:113–126. [PubMed: 16520830]
- Lepore AC, Maragakis NJ. Stem cell transplantation for spinal cord neurodegeneration. *Methods Mol Biol*. 2011; 793:479–493. [PubMed: 21913120]
- Lepore AC, Neuhuber B, Connors TM, Han SS, Liu Y, Daniels MP, Rao MS, Fischer I. Long-term fate of neural precursor cells following transplantation into developing and adult CNS. *Neuroscience*. 2006; 139:513–530. [PubMed: 16458439]
- Lepore AC, O'Donnell J, Bonner JF, Paul C, Miller ME, Rauck B, Kushner RA, Rothstein JD, Fischer I, Maragakis NJ. Spatial and temporal changes in promoter activity of the astrocyte glutamate transporter GLT1 following traumatic spinal cord injury. *J Neurosci Res*. 2011a; 89:1001–1017. [PubMed: 21488085]
- Lepore AC, O'Donnell J, Kim AS, Williams T, Tuteja A, Rao MS, Kelley LL, Campanelli JT, Maragakis NJ. Human glial-restricted progenitor transplantation into cervical spinal cord of the SOD1G93A mouse model of ALS. *PLoS One*. 2011b; 6
- Lepore AC, O'Donnell J, Kim AS, Yang EJ, Tuteja A, Haidet-Phillips A, O'Banion CP, Maragakis NJ. Reduction in expression of the astrocyte glutamate transporter, GLT1, worsens functional and histological outcomes following traumatic spinal cord injury. *Glia*. 2011c; 59:1996–2005. [PubMed: 21882244]
- Lepore AC, Rauck B, Dejea C, Pardo AC, Rao MS, Rothstein JD, Maragakis NJ. Focal transplantation-based astrocyte replacement is neuroprotective in a model of motor neuron disease. *Nature neuroscience*. 2008b; 11:1294–1301. [PubMed: 18931666]
- Li K, Javed E, Hala TJ, Sannie D, Regan KA, Maragakis NJ, Wright MC, Poulsen DJ, Lepore AC. Transplantation of Glial Progenitors That Overexpress Glutamate Transporter GLT1 Preserves Diaphragm Function Following Cervical SCI. *Mol Ther*. 2014a
- Li K, Nicaise C, Sannie D, Hala TJ, Javed E, Parker JL, Putatunda R, Regan KA, Suain V, Brion JP, Rhoderick F, Wright MC, Poulsen DJ, Lepore AC. Overexpression of the Astrocyte Glutamate Transporter GLT1 Exacerbates Phrenic Motor Neuron Degeneration, Diaphragm Compromise, and Forelimb Motor Dysfunction following Cervical Contusion Spinal Cord Injury. *J Neurosci*. 2014b; 34:7622–7638. [PubMed: 24872566]
- Liu D, Thangnipon W, McAdoo DJ. Excitatory amino acids rise to toxic levels upon impact injury to the rat spinal cord. *Brain research*. 1991; 547:344–348. [PubMed: 1884213]
- Maragakis NJ, Rothstein JD. Glutamate transporters: animal models to neurologic disease. *Neurobiol Dis*. 2004; 15:461–473. [PubMed: 15056453]
- Maragakis NJ, Rothstein JD. Mechanisms of Disease: astrocytes in neurodegenerative disease. *Nat Clin Pract Neurol*. 2006; 2:679–689. [PubMed: 17117171]
- McDonald JW, Becker D. Spinal cord injury: promising interventions and realistic goals. *Am J Phys Med Rehabil*. 2003; 82:S38–S49. [PubMed: 14502038]
- Mitsui T, Shumsky JS, Lepore AC, Murray M, Fischer I. Transplantation of neuronal and glial restricted precursors into contused spinal cord improves bladder and motor functions, decreases thermal hypersensitivity, and modifies intraspinal circuitry. *J Neurosci*. 2005; 25:9624–9636. [PubMed: 16237167]
- Neuhuber B, Timothy Himes B, Shumsky JS, Gallo G, Fischer I. Axon growth and recovery of function supported by human bone marrow stromal cells in the injured spinal cord exhibit donor variations. *Brain research*. 2005; 1035:73–85. [PubMed: 15713279]
- Nicaise C, Frank DM, Hala TJ, Authelet M, Pochet R, Adriaens D, Brion JP, Wright MC, Lepore AC. Early phrenic motor neuron loss and transient respiratory abnormalities after unilateral cervical spinal cord contusion. *Journal of neurotrauma*. 2013; 30:1092–1099. [PubMed: 23534670]

- Nicaise C, Hala TJ, Frank DM, Parker JL, Authelet M, Leroy K, Brion JP, Wright MC, Lepore AC. Phrenic motor neuron degeneration compromises phrenic axonal circuitry and diaphragm activity in a unilateral cervical contusion model of spinal cord injury. *Experimental neurology*. 2012; 235:539–552. [PubMed: 22465264]
- Nori S, Okada Y, Yasuda A, Tsuji O, Takahashi Y, Kobayashi Y, Fujiyoshi K, Koike M, Uchiyama Y, Ikeda E, Toyama Y, Yamanaka S, Nakamura M, Okano H. Grafted human-induced pluripotent stem-cell-derived neurospheres promote motor functional recovery after spinal cord injury in mice. *Proc Natl Acad Sci U S A*. 2011; 108:16825–16830. [PubMed: 21949375]
- Nutt SE, Chang EA, Suhr ST, Schlosser LO, Mondello SE, Moritz CT, Cibelli JB, Horner PJ. Caudalized human iPSC-derived neural progenitor cells produce neurons and glia but fail to restore function in an early chronic spinal cord injury model. *Experimental neurology*. 2013; 248:491–503. [PubMed: 23891888]
- Olsen ML, Campbell SC, McFerrin MB, Floyd CL, Sontheimer H. Spinal cord injury causes a widespread, persistent loss of Kir4.1 and glutamate transporter 1: benefit of 17 beta-oestradiol treatment. *Brain*. 2010; 133:1013–1025. [PubMed: 20375134]
- Panter SS, Yum SW, Faden AI. Alteration in extracellular amino acids after traumatic spinal cord injury. *Annals of neurology*. 1990; 27:96–99. [PubMed: 2301932]
- Park E, Velumian AA, Fehlings MG. The role of excitotoxicity in secondary mechanisms of spinal cord injury: a review with an emphasis on the implications for white matter degeneration. *J Neurotrauma*. 2004; 21:754–774. [PubMed: 15253803]
- Pekny M, Nilsson M. Astrocyte activation and reactive gliosis. *Glia*. 2005; 50:427–434. [PubMed: 15846805]
- Perego C, Vanoni C, Bossi M, Massari S, Basudev H, Longhi R, Pietrini G. The GLT-1 and GLAST glutamate transporters are expressed on morphologically distinct astrocytes and regulated by neuronal activity in primary hippocampal cocultures. *J Neurochem*. 2000; 75:1076–1084. [PubMed: 10936189]
- Pomeshchik Y, Puttonen KA, Kidin I, Ruponen M, Lehtonen S, Malm T, Akesson E, Hovatta O, Koistinaho J. Transplanted human iPSC-derived neural progenitor cells do not promote functional recovery of pharmacologically immunosuppressed mice with contusion spinal cord injury. *Cell Transplant*. 2014
- Putatunda R, Hala TJ, Chin J, Lepore AC. Chronic at-level thermal hyperalgesia following rat cervical contusion spinal cord injury is accompanied by neuronal and astrocyte activation and loss of the astrocyte glutamate transporter, GLT1, in superficial dorsal horn. *Brain research*. 2014; 18:64–79. [PubMed: 24833066]
- Romanyuk N, Amemori T, Turnovcova K, Prochazka P, Onteniente B, Sykova E, Jendelova P. Beneficial effect of human induced pluripotent stem cell-derived neural precursors in spinal cord injury repair. *Cell Transplant*. 2014
- Salewski RP, Eftekharpour E, Fehlings MG. Are induced pluripotent stem cells the future of cell-based regenerative therapies for spinal cord injury? *J Cell Physiol*. 2010; 222:515–521. [PubMed: 20020443]
- Sandrow-Feinberg HR, Izzi J, Shumsky JS, Zhukareva V, Houle JD. Forced exercise as a rehabilitation strategy after unilateral cervical spinal cord contusion injury. *J Neurotrauma*. 2009; 26:721–731. [PubMed: 19489718]
- Sandrow-Feinberg HR, Zhukareva V, Santi L, Miller K, Shumsky JS, Baker DP, Houle JD. PEGylated interferon-beta modulates the acute inflammatory response and recovery when combined with forced exercise following cervical spinal contusion injury. *Experimental neurology*. 2010; 223:439–451. [PubMed: 20109445]
- Sandrow HR, Shumsky JS, Amin A, Houle JD. Aspiration of a cervical spinal contusion injury in preparation for delayed peripheral nerve grafting does not impair forelimb behavior or axon regeneration. *Experimental neurology*. 2008; 210:489–500. [PubMed: 18295206]
- Sareen D, Gowing G, Sahabian A, Staggenborg K, Paradis R, Avalos P, Latter J, Ornelas L, Garcia L, Svendsen CN. Human induced pluripotent stem cells are a novel source of neural progenitor cells (iNPCs) that migrate and integrate in the rodent spinal cord. *J Comp Neurol*. 2014; 522:2707–2728. [PubMed: 24610630]

- Shanmuganathan K, Gullapalli RP, Zhuo J, Mirvis SE. Diffusion tensor MR imaging in cervical spine trauma. *AJNR Am J Neuroradiol*. 2008; 29:655–659. [PubMed: 18238846]
- Simone C, Nizzardo M, Rizzo F, Ruggieri M, Riboldi G, Salani S, Bucchia M, Bresolin N, Comi GP, Corti S. iPSC-Derived neural stem cells act via kinase inhibition to exert neuroprotective effects in spinal muscular atrophy with respiratory distress type 1. *Stem Cell Reports*. 2014; 3:297–311. [PubMed: 25254343]
- Smith GM, Miller RH, Silver J. Changing role of forebrain astrocytes during development, regenerative failure, and induced regeneration upon transplantation. *J Comp Neurol*. 1986; 251:23–43. [PubMed: 3760257]
- Stamegna JC, Felix MS, Roux-Peyronnet J, Rossi V, Feron F, Gauthier P, Matarazzo V. Nasal OEC transplantation promotes respiratory recovery in a subchronic rat model of cervical spinal cord contusion. *Experimental neurology*. 2011; 229:120–131. [PubMed: 20633558]
- Steward O, Sharp KG, Yee KM, Hatch MN, Bonner JF. Characterization of ectopic colonies that form in widespread areas of the nervous system with neural stem cell transplants into the site of a severe spinal cord injury. *J Neurosci*. 2014; 34:14013–14021. [PubMed: 25319698]
- Strakowski JA, Pease WS, Johnson EW. Phrenic nerve stimulation in the evaluation of ventilator-dependent individuals with C4- and C5-level spinal cord injury. *Am J Phys Med Rehabil*. 2007; 86:153–157. [PubMed: 17251697]
- Stys PK. White matter injury mechanisms. *Curr Mol Med*. 2004; 4:113–130. [PubMed: 15032708]
- Takahashi K, Okita K, Nakagawa M, Yamanaka S. Induction of pluripotent stem cells from fibroblast cultures. *Nat Protoc*. 2007a; 2:3081–3089. [PubMed: 18079707]
- Takahashi K, Tanabe K, Ohnuki M, Narita M, Ichisaka T, Tomoda K, Yamanaka S. Induction of pluripotent stem cells from adult human fibroblasts by defined factors. *Cell*. 2007b; 131:861–872. [PubMed: 18035408]
- Taylor CJ, Bolton EM, Bradley JA. Immunological considerations for embryonic and induced pluripotent stem cell banking. *Philos Trans R Soc Lond B Biol Sci*. 2011; 366:2312–2322. [PubMed: 21727137]
- Tsuji O, Miura K, Okada Y, Fujiyoshi K, Mukaino M, Nagoshi N, Kitamura K, Kumagai G, Nishino M, Tomisato S, Higashi H, Nagai T, Katoh H, Kohda K, Matsuzaki Y, Yuzaki M, Ikeda E, Toyama Y, Nakamura M, Yamanaka S, Okano H. Therapeutic potential of appropriately evaluated safe-induced pluripotent stem cells for spinal cord injury. *Proc Natl Acad Sci U S A*. 2010; 107:12704–12709. [PubMed: 20615974]
- Watson JL, Hala TJ, Putatunda R, Sannie D, Lepore AC. Persistent at-level thermal hyperalgesia and tactile allodynia accompany chronic neuronal and astrocyte activation in superficial dorsal horn following mouse cervical contusion spinal cord injury. *PLoS One*. 2014; 9:e109099. [PubMed: 25268642]
- Wright MC, Cho WJ, Son YJ. Distinct patterns of motor nerve terminal sprouting induced by ciliary neurotrophic factor vs. botulinum toxin. *J Comp Neurol*. 2007; 504:1–16. [PubMed: 17614103]
- Wright MC, Potluri S, Wang X, Dentcheva E, Gautam D, Tessler A, Wess J, Rich MM, Son YJ. Distinct muscarinic acetylcholine receptor subtypes contribute to stability and growth, but not compensatory plasticity, of neuromuscular synapses. *J Neurosci*. 2009; 29:14942–14955. [PubMed: 19940190]
- Wright MC, Son YJ. Ciliary neurotrophic factor is not required for terminal sprouting and compensatory reinnervation of neuromuscular synapses: re-evaluation of CNTF null mice. *Experimental neurology*. 2007; 205:437–448. [PubMed: 17445802]
- Xu GY, Hughes MG, Ye Z, Hulsebosch CE, McAdoo DJ. Concentrations of glutamate released following spinal cord injury kill oligodendrocytes in the spinal cord. *Experimental neurology*. 2004; 187:329–336. [PubMed: 15144859]
- Xu GY, Hughes MG, Zhang L, Cain L, McAdoo DJ. Administration of glutamate into the spinal cord at extracellular concentrations reached post-injury causes functional impairments. *Neuroscience letters*. 2005; 384:271–276. [PubMed: 15925447]
- Zimmer MB, Nantwi K, Goshgarian HG. Effect of spinal cord injury on the respiratory system: basic research and current clinical treatment options. *The journal of spinal cord medicine*. 2007; 30:319–330. [PubMed: 17853653]

Zimmermann A, Preynat-Seauve O, Tiercy JM, Krause KH, Villard J. Haplotype-based banking of human pluripotent stem cells for transplantation: potential and limitations. *Stem Cells Dev.* 2012; 21:2364–2373. [PubMed: 22559254]

Author Manuscript

Author Manuscript

Author Manuscript

Author Manuscript

Highlights

- We transplanted human iPS cell-derived astrocytes (hIPSA) in cervical contusion SCI
- Transplants showed robust long-term survival and efficient astrocyte differentiation
- We engineered hIPSA transplants to overexpress astrocyte glutamate transporter GLT1
- GLT1-hIPSA reduced lesion size, motor neuron loss and diaphragm denervation
- GLT1-hIPSA transplants also partially preserved diaphragmatic respiratory function

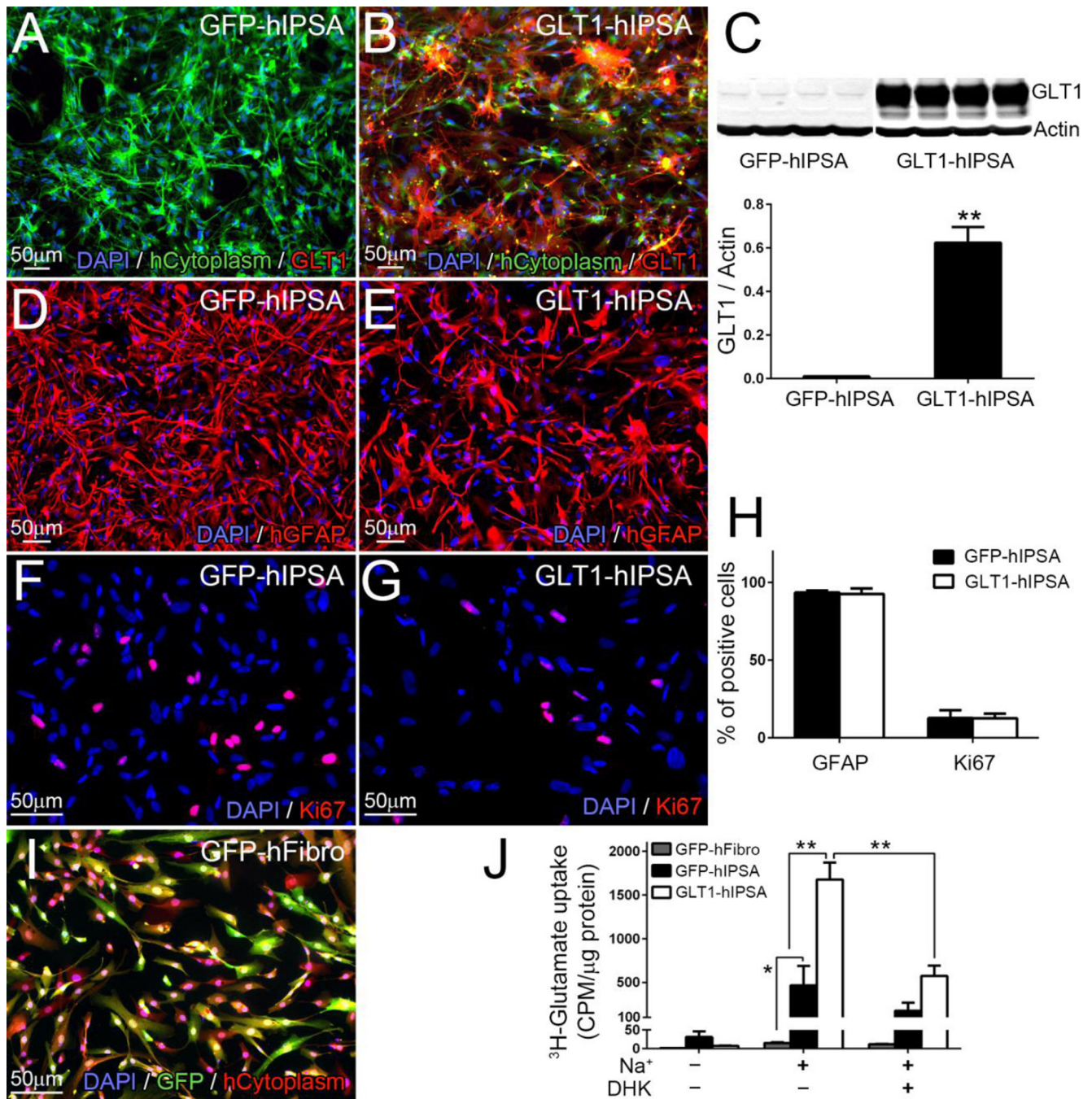


Figure 1. *In vitro* characterization of human iPS cell-derived astrocytes (hIPSA)
Cells were transduced with lentivirus (LV)-GFP or LV-GLT1-GFP to generate control GFP-hIPSA and GLT1-overexpressing hIPSA (GLT1-hIPSA), respectively. Human cytoplasm⁺ GFP-hIPSA expressed little-to-no GLT1 protein (**A**), while GLT1-hIPSA expressed high levels of GLT1 protein *in vitro* (**B**), which was further confirmed with immunoblotting analysis (**C**, *lower*: quantification result). Following infection with either virus, astrocyte differentiation was determined by the percentage of cells expressing the astrocyte lineage marker, GFAP (**D–E**). Proliferation was determined by the percentage of

cells expressing the proliferation marker, Ki67 (**F–G**). Quantification results of cell differentiation and proliferation are shown in (**H**). Human fibroblasts, which were transduced with LV-GFP vector (GFP-hFibro) (**I**), were used as non-gial control in the glutamate uptake assay and *in vivo* transplantation experiments. ^3H -glutamate uptake assay was performed to detect GLT1 function. GLT1-hIPSAAs showed a large increase in Na^+ dependent glutamate uptake compared to GFP-hFibro and GFP-hIPSAAs. This increased uptake was blocked with GLT1 specific inhibitor, DHK, at the concentration of 100 $\mu\text{mol/L}$ (**J**). Results were expressed as means \pm SEM. * $p < 0.05$, ** $p < 0.01$. n = 4 per group for GLT1 western blotting quantification analysis; n = 4 per group for cell differentiation and proliferation analysis; n = 4 per group for ^3H -glutamate uptake assay.

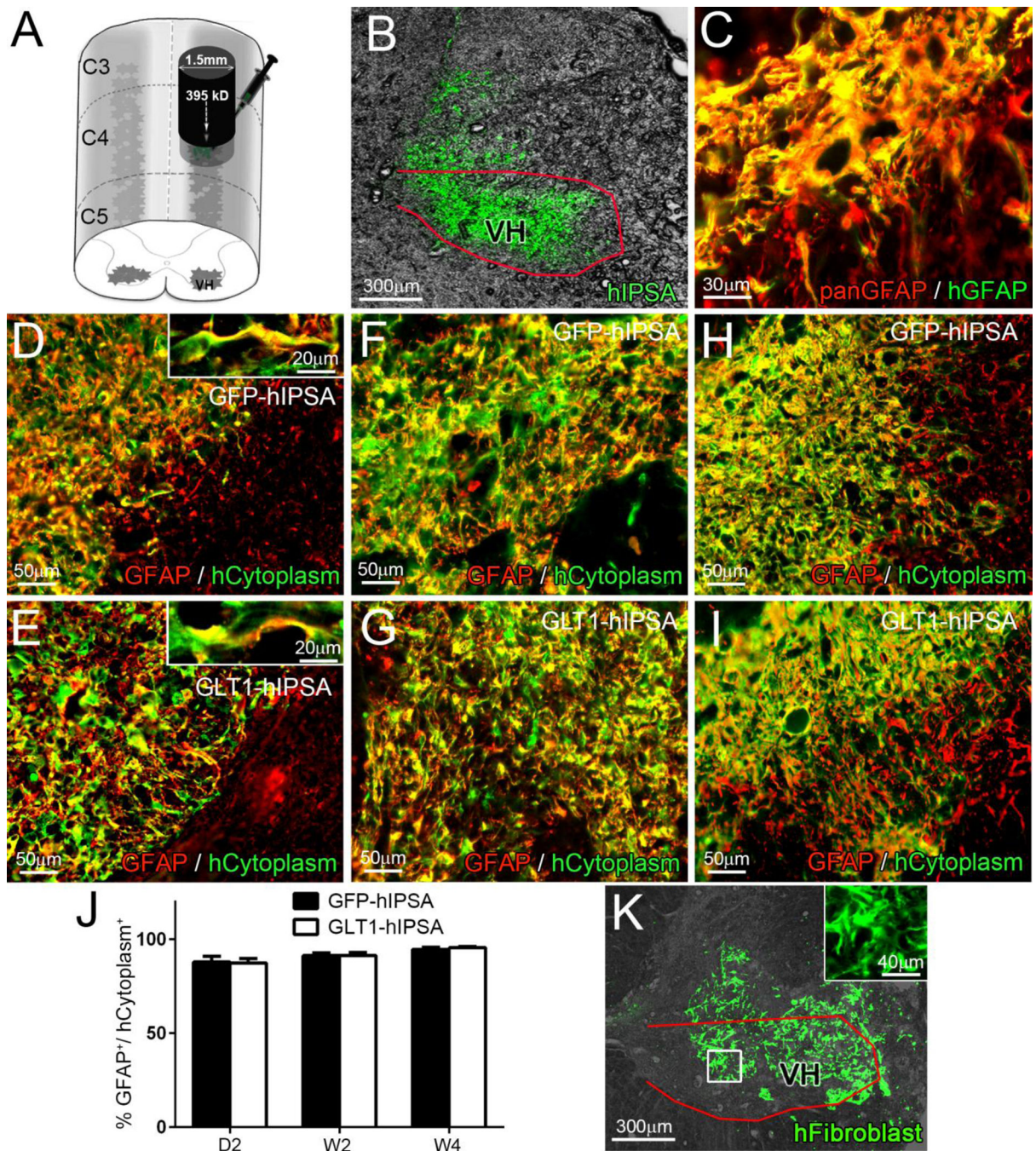


Figure 2. Human iPSC transplants robustly survived, differentiated into astrocytes and localized to the ventral horn following rat cervical contusion SCI

Immediately following unilateral C4 contusion SCI, we injected GFP-hIPSA, GLT1-hIPSA or GFP-hFibro directly into the ventral horn (VH) at locations just rostral and caudal to the contusion site (A). GFP fluorescence indicated that the transplanted hIPSA were delivered to the ventral horn (B). Double-labeling with pan-GFAP antibody and a human GFAP specific antibody confirmed that all human GFAP⁺ cells were also pan-GFAP⁺ (C). Double immunostaining for pan-GFAP and human cytoplasm marker was performed on

spinal cord sections from the GFP-hIPSA (**D, F, H**) and GLT1-hIPSA (**E, G, I**) groups at day 2 (**D-E**), week 2 (**F-G**) and week 4 (**H-I**) post-injury/transplantation to quantify astrocyte differentiation by transplanted cells (**J**). We used LV-GFP transduced human fibroblasts (GFP-hFibro) as a non-glial cell control (**K**, *inset*: high magnification). Results were expressed as means \pm SEM. n = 3 per group per time point for transplanted cell differentiation analysis. Red outlines in panels B and K denote the ventral horn.

Author Manuscript

Author Manuscript

Author Manuscript

Author Manuscript

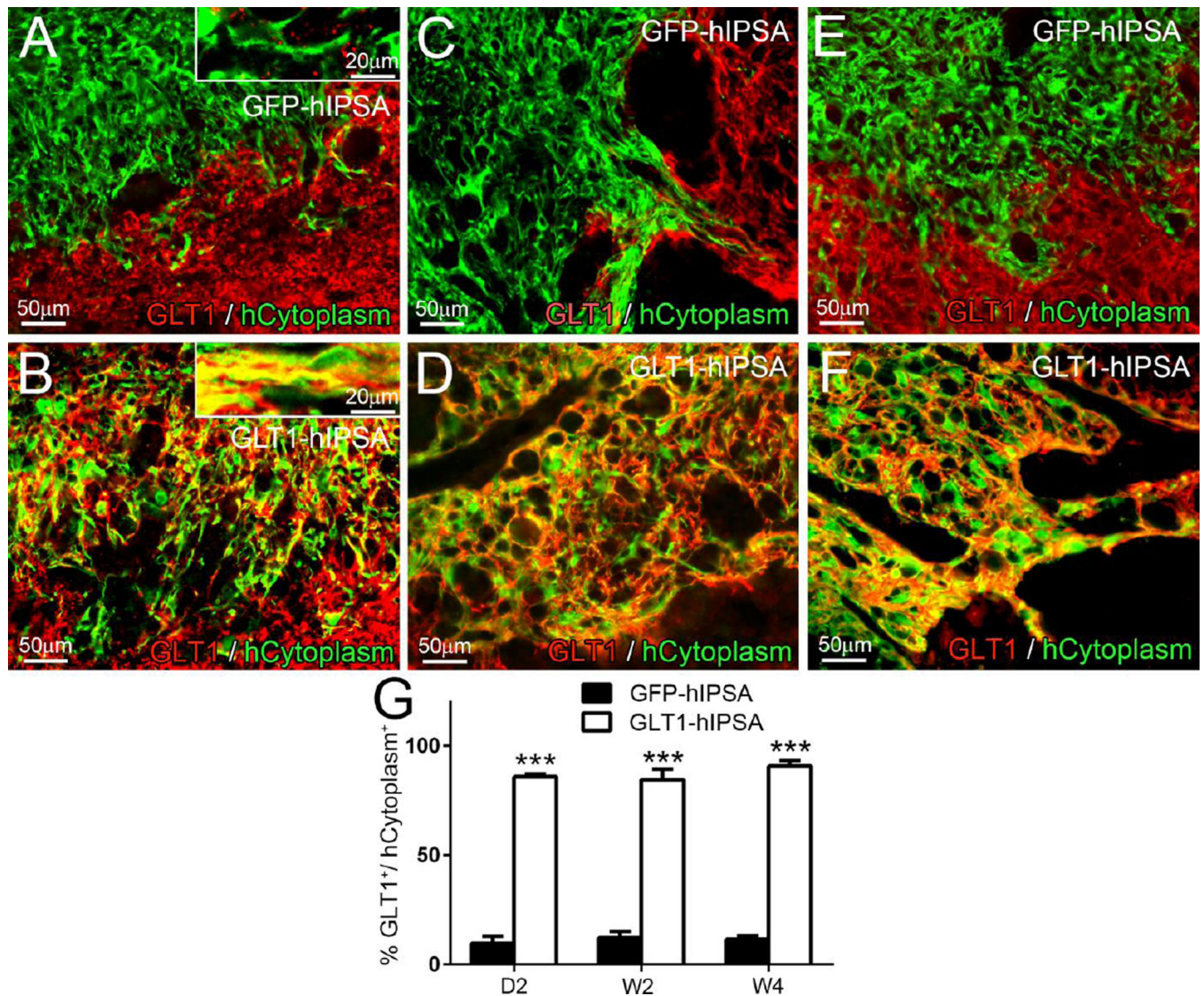


Figure 3. GLT1-hIPSA transplants expresses GLT1 in the ventral horn following rat cervical contusion SCI

Double immunostaining for GLT1 and human cytoplasm was performed on spinal cord sections from the GFP-hIPSA (A, C, E) and GLT1-hIPSA (B, D, F) groups at day 2 (A–B), week 2 (C–D) and week 4 (E–F) post-injury/transplantation to assess GLT1 expression by transplanted cells *in vivo* (G). Results were expressed as means \pm SEM. *** p <0.001. $n = 3$ per group per time point for *in vivo* GLT1 expression analysis.

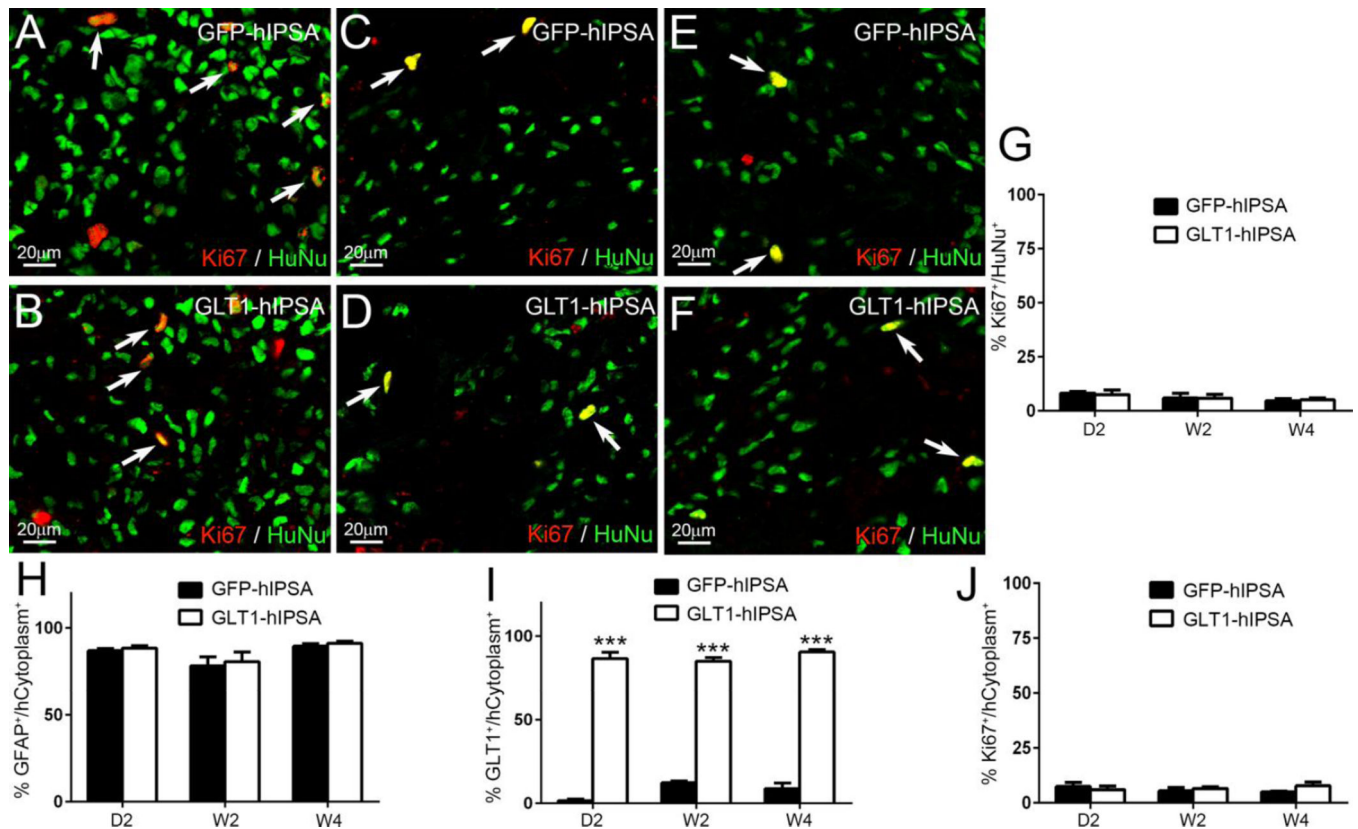


Figure 4. Transplanted hiPSAs showed limited proliferation and did not form tumors
 Double immunostaining for the proliferation marker Ki67 with human nuclei (HuNu) was performed on spinal cord sections from the GFP-hiPSA (A, C, E) and GLT1-hiPSA (B, D, F) groups at D2 (A–B), W2 (C–D) and W4 (E–F) post-transplantation, and quantification results are shown in (G). Tumor formation was never observed. We conducted similar *in vivo* characterization of hiPSA fate following transplantation into the mouse spinal cord immediately following unilateral cervical contusion SCI. The majority of transplant-derived cells were differentiated GFAP⁺ astrocytes (H). Control GFP-hiPSAs did not express GLT1, while overexpression resulted in the majority of transplant-derived astrocytes expressing GLT1 (I). Less than 10% of transplant-derived cells continued to proliferate at D2, W2 and W4 (J). Results were expressed as means \pm SEM. *** p <0.001. n = 3 per group per time point in cell fate analysis.

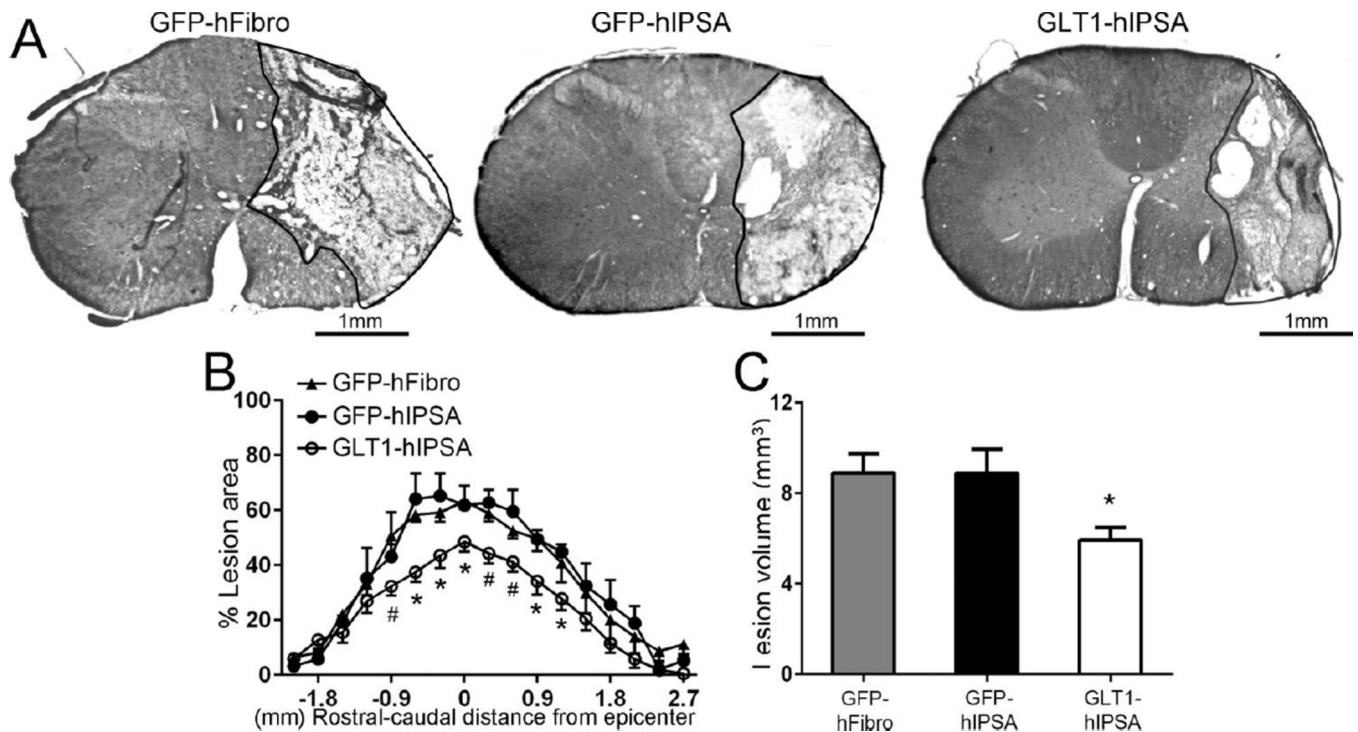


Figure 5. GLT1 overexpressing hIPSA transplants reduced lesion size following cervical contusion SCI

At 4 weeks post-injury, we quantified Cresyl-violet stained transverse sections of the cervical spinal cord for the degree of ipsilesional tissue sparing by calculating the percentage of total ipsilateral hemi-cord area comprised of damaged tissue (A). Lesion area (B) and total lesion volume (C) analysis (combined for both white and gray matter) revealed that GLT1-hIPSA transplants significantly reduced lesion size at multiple locations surrounding the epicenter compared to both human fibroblast and control GFP-hIPSA transplant groups. Results were expressed as means \pm SEM. # $p < 0.05$, GLT1-hIPSA group versus GFP-hIPSA group only; * $p < 0.05$, GLT1-hIPSA group versus both control groups. $n = 6$ per group for lesion area and volume analysis.

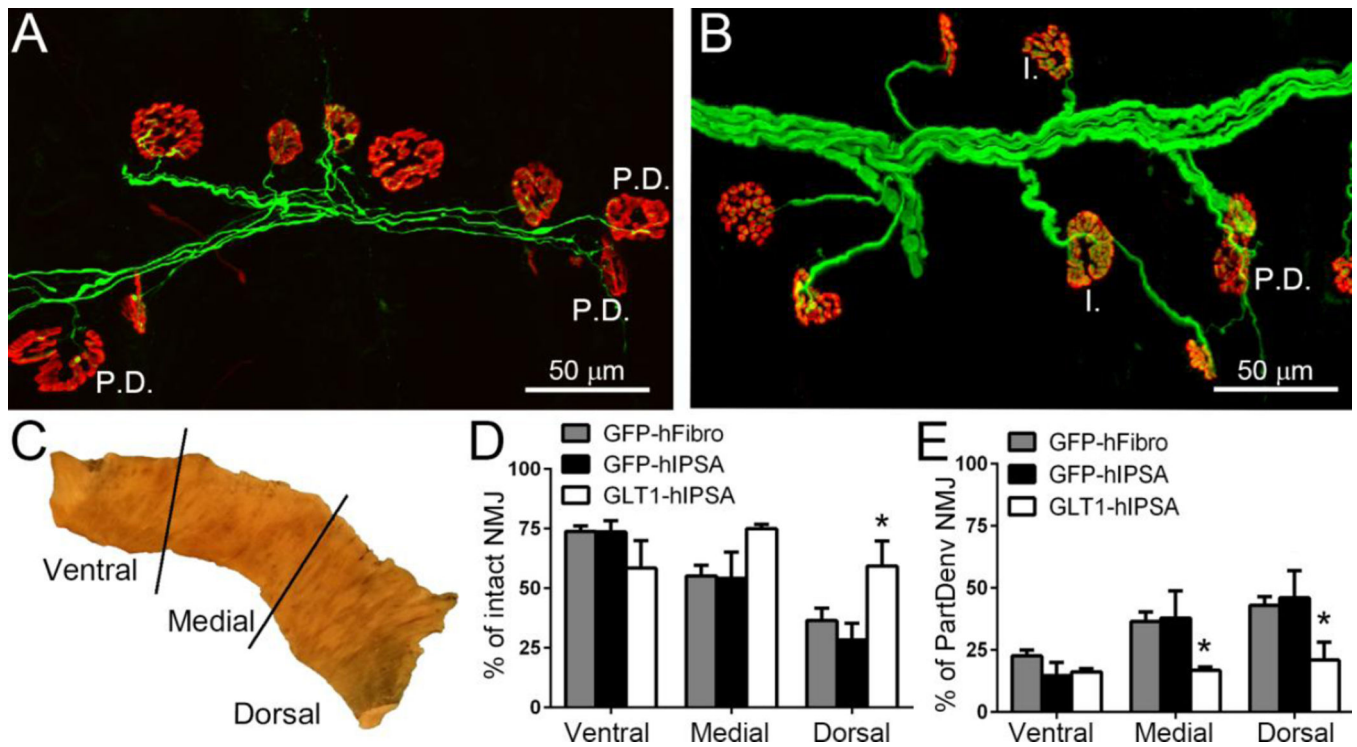


Figure 6. GLT1 overexpressing hIPSA astrocyte transplants preserved diaphragm innervation by phrenic motor neurons following cervical contusion SCI

To examine pathological alterations at the diaphragm NMJ, hemi-diaphragm muscle ipsilateral to the contusion from the GFP-hFibro (A), GFP-hIPSA and GLT1-hIPSA (B) groups was examined at 4 weeks post-injury/transplantation. Individual NMJs were characterized as: intact (I.) and partially denervated (P.D.). For analysis, the hemi-diaphragm was divided into three anatomical regions (ventral, medial and dorsal) (C). At the dorsal region of the hemi-diaphragm, the percentage of intact NMJs in the GLT1-hIPSA group was significant greater than both control groups (D). GLT1-hIPSA transplants significantly reduced the percentage of partially denervated NMJs in the medial and dorsal hemi-diaphragm regions compared to both control groups (E). Results were expressed as means \pm SEM. * $p < 0.05$, GLT1-hIPSA group versus both control groups. $n = 4-6$ per group for NMJ analysis.

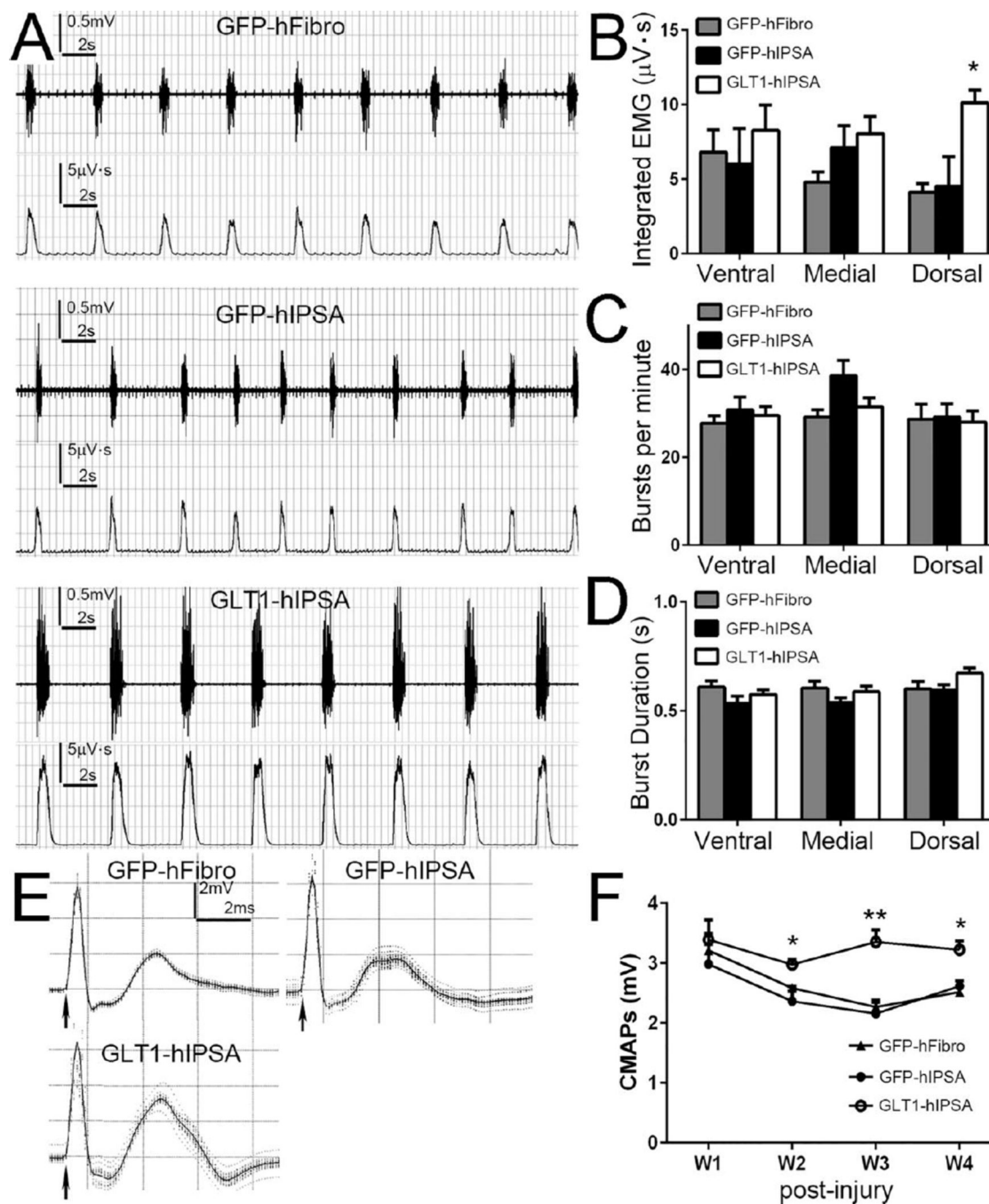


Figure 7. GLT1 overexpressing hIPSA transplants preserved diaphragm function following cervical contusion SCI

Spontaneous EMG recordings from ipsilateral hemi-diaphragm were obtained at 4 weeks post-injury/transplantation (A, *upper*: raw EMG; *lower*: integrated EMG). Integrated EMG amplitude (B), burst frequency (C), and burst duration (D) were analyzed. Following supramaximal phrenic nerve stimulation, we obtained compound muscle action potential (CMAP) recordings from the ipsilateral hemi-diaphragm using a surface electrode (E). CMAP amplitudes at different time points post-injury were analyzed (F). Results were

expressed as means \pm SEM. * $p < 0.05$, ** $p < 0.01$, GLT1-hIPSA group versus both control groups. n = 6 per group for EMG and CMAP analysis.

Author Manuscript

Author Manuscript

Author Manuscript

Author Manuscript